

ACS **APPLIED**
ENERGY MATERIALS

March 23, 2026
Volume 9
Number 6
pubs.acs.org/acsaem



 **ACS Publications**
Most Trusted. Most Cited. Most Read.

www.acs.org



About the Cover:

This all-in-one architecture unifies flexible energy storage with multifunctional sensing. With the combination of diverse materials and machine learning for data processing, the platform interprets intrinsic electrochemical fluctuations as meaningful environmental signals. This integration enables self-powered, real-time monitoring for next-generation wearable electronics and smart systems. [View the article.](#)

[Download Cover](#)

In this issue:

- » [Comments](#)
- » [Reviews](#)
- » [Letters](#)
- » [Articles](#)
- » [Additions and Corrections](#)
- » [Mastheads](#)



Sort By:

Page

COMMENTS

Comments on “Interlayer Atomic Voids by Partial Cesium Defect in Layered Titanate Activate Photo(electro)catalytic H₂ and O₂ Generation”

Tosapol Maluangnont*

ACS Applied Energy Materials 2026, 9, 6, 2928-2930 (Comment) [Open Access](#)

Publication Date (Web): March 2, 2026



[Abstract](#)

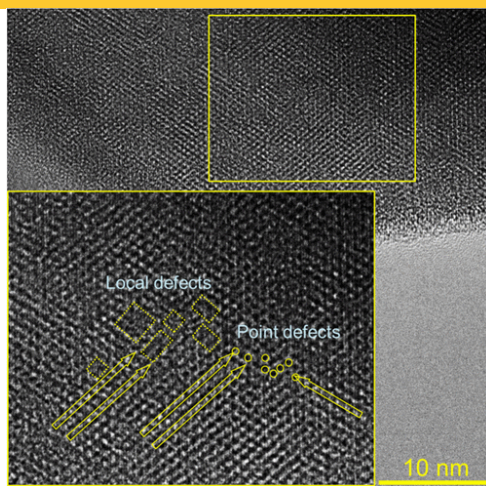


[Full text](#)



[PDF](#)

▼ **ABSTRACT**



Re

Response to the Comment by T. Maluangnont on “Interlayer Atomic Voids by Partial Cesium Defect in Layered Titanate Activate Photo(electro)catalytic H₂ and O₂ Generation”

Esmail Doustkhah*, José Julio Gutiérrez Moreno, and Sarp Kaya*

ACS Applied Energy Materials 2026, 9, 6, 2931-2935 (Comment) Subscribed

Publication Date (Web): March 5, 2026

 Abstract

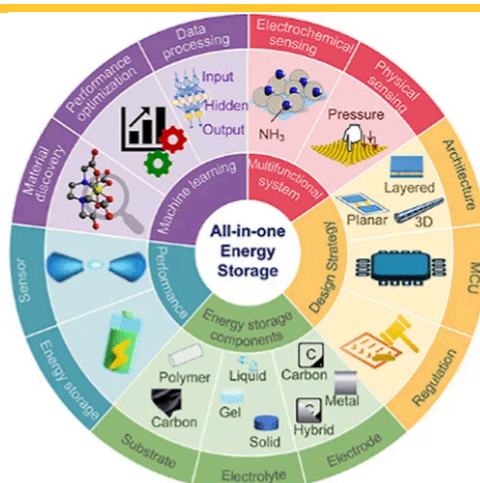
 Full text

 PDF

▼ ABSTRACT

ADVERTISEMENT

REVIEWS



Integrated Energy Storage with Smart Sensing for Flexible Electronics

Soon Poh Lee, Kwok Feng Chong, Eng Hock Lim, Chun Hui Tan*, and Pei Song Chee*

ACS Applied Energy Materials 2026, 9, 6, 2936-2962 (Review) Subscribed

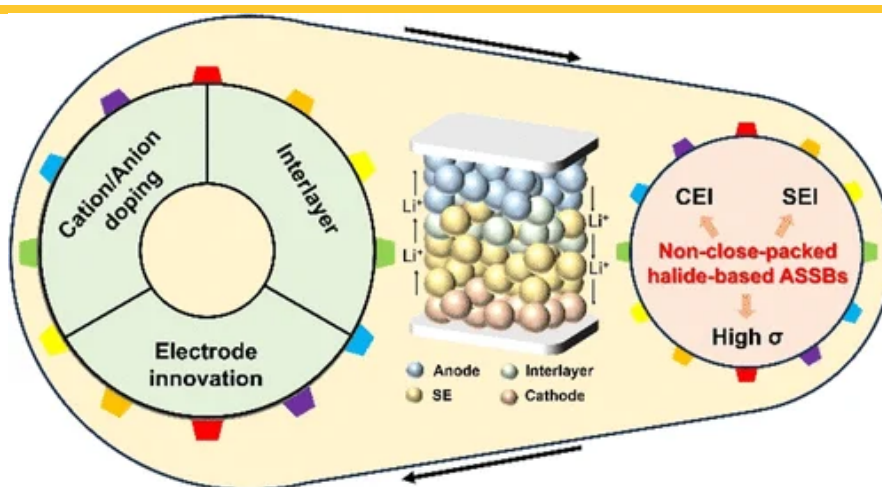
Publication Date (Web): February 19, 2026

 Abstract

 Full text

 PDF

✓ ABSTRACT



Advancing Interface Engineering for Non-Close-Packed Halide-Based All-Solid-State Lithium Batteries

Kai Zhang, Songjia Kong, Keqi Chen, Shumin Zhang*, Yanguang Li*, and Feipeng Zhao*

ACS Applied Energy Materials 2026, 9, 6, 2963-2974 (Review) Subscribed

Publication Date (Web): March 3, 2026

 Abstract

 Full text

 PDF

✓ ABSTRACT



Fluorspar



Fluorinated chemicals

Fluorinated Lithium Salt from Fluorspar Bypassing HF: An Outlook on Related Green Fluorine Chemical Industry

Meng Ge*, Yitian Chen, Jian Liu, Yiyang Zhang, and Lei Yu*

ACS Applied Energy Materials 2026, 9, 6, 2975-2981 (Review) [Subscribed](#)

Publication Date (Web): March 11, 2026

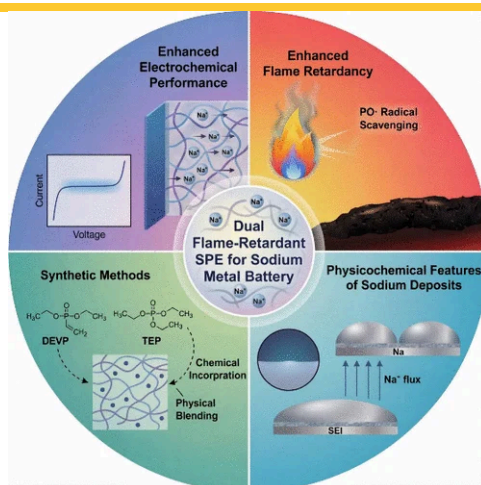
Abstract

Full text

PDF

✓ ABSTRACT

LETTERS



Introducing Flame Retardancy to Solid-State Electrolytes for Reliable and Safe Sodium–Metal Anode Batteries

Yuzheng Xie and Ruoqian Lin*

ACS Applied Energy Materials 2026, 9, 6, 2982-2991 (Letter) [Subscribed](#)

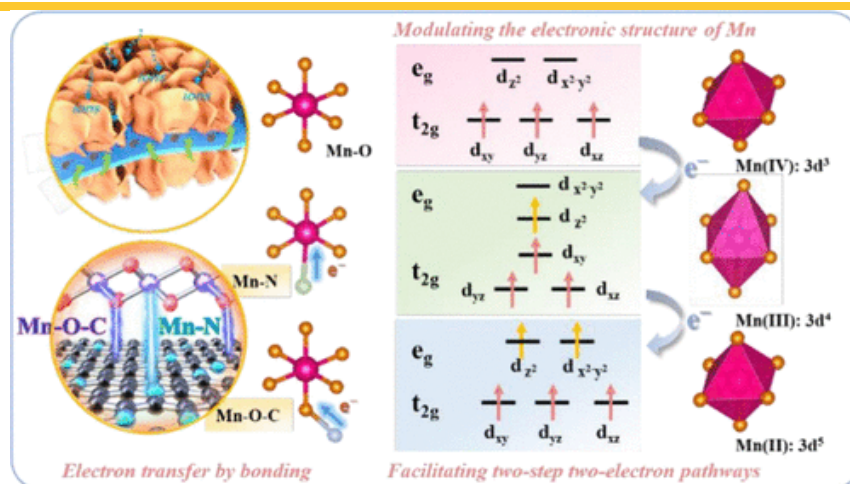
Publication Date (Web): March 10, 2026

Abstract

Full text

PDF

✓ ABSTRACT



Regulating the Electronic Structure of Mn via Chemical Bonding to Activate the Two-Electron Reaction of δ -MnO₂ for Zinc-Ion Batteries

Xinyue Wu, Jinze Zhang, Gaini Zhang*, Yanyan Cao, Xinyu Hua, Yuhui Xu, Jianhua Zhang, Qinting Jiang, Huijun Yang, Yangyang Luo, Xuexia Song, Jingjing Wang, Wenbin Li, and Xifei Li*

ACS Applied Energy Materials 2026, 9, 6, 2992-3004 (Article) [Subscribed](#)

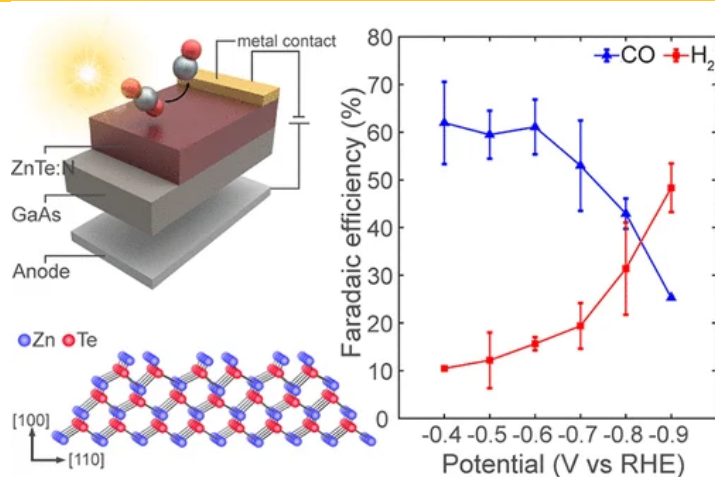
Publication Date (Web): March 4, 2026

[Abstract](#)

[Full text](#)

[PDF](#)

✓ ABSTRACT



Investigation of CO₂-to-CO Conversion by Cocatalyst-Free Epitaxial ZnTe Photocathodes

Lily Shiao, Sol A Lee, Soonho Kwon, Phillip Jahelka, and Harry A. Atwater*

ACS Applied Energy Materials 2026, 9, 6, 3005-3015 (Article) Subscribed

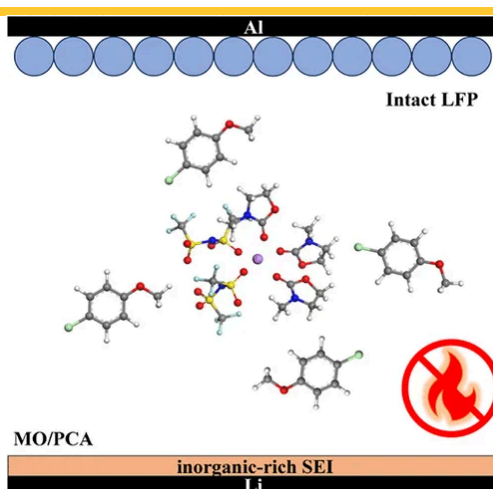
Publication Date (Web): March 6, 2026

 Abstract

 Full text

 PDF

✓ ABSTRACT



Enhancing Cycling Stability of Lithium Metal Batteries with Nonflammable Electrolytes Using 4-Chloroanisole as a Cosolvent

Zhenghong Yan, Zhenye Zhu*, Gefeng Li, Liang Zhou, Yuhao Wang, Guanghao Mao, Xinyi He, Juntao Lin, and Rongshu Zhu*

ACS Applied Energy Materials 2026, 9, 6, 3016-3027 (Article) Subscribed

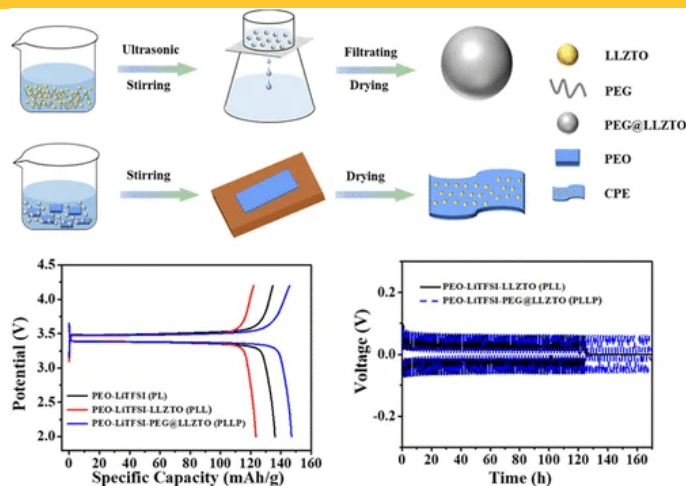
Publication Date (Web): March 3, 2026

 Abstract

 Full text

 PDF

✓ ABSTRACT



Surface Engineering of $\text{Li}_{6.4}\text{La}_3\text{Zr}_{1.4}\text{Ta}_{0.6}\text{O}_{12}$ via Poly(ethylene glycol) Functionalization for High-Performance Poly(ethylene oxide)-Based Composite Electrolytes in All-Solid-State Lithium Metal Batteries

Jiangtao Zhang, Ruochen Xu*, Jiayun Wang, Zhouting Sun, Panxing Bai, and Mingyi Liu*

ACS Applied Energy Materials 2026, 9, 6, 3028-3037 (Article) [Subscribed](#)

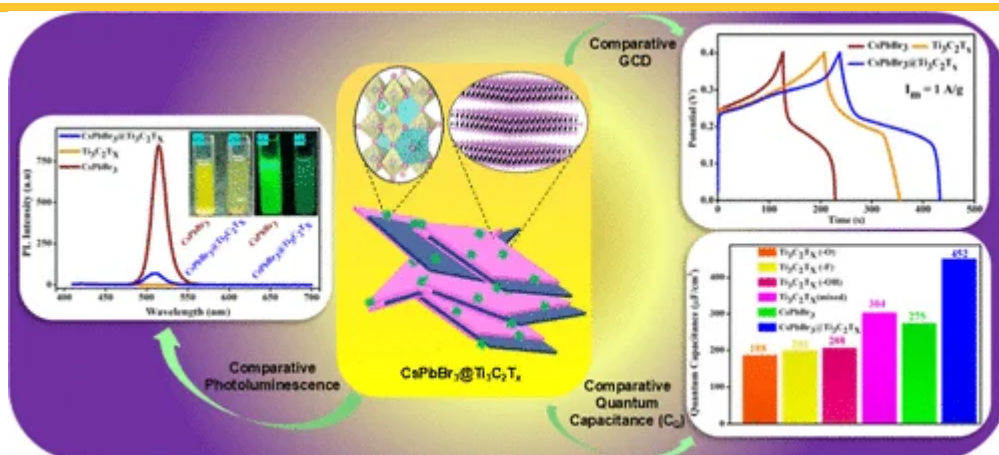
Publication Date (Web): March 2, 2026

[Abstract](#)

[Full text](#)

[PDF](#)

ABSTRACT



Hierarchically Structured $\text{CsPbBr}_3@ \text{Ti}_3\text{C}_2\text{T}_x$ Nanohybrid Frameworks for High-Performance Supercapacitors

Priyanka, Avinash Rundla, Mahaveer Singh, Bheem Kumar, Vikash Mishra, and Kedar Singh*

ACS Applied Energy Materials 2026, 9, 6, 3038-3052 (Article) Subscribed

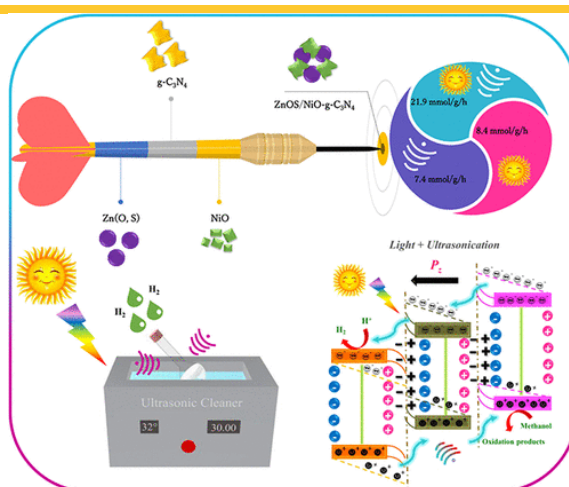
Publication Date (Web): March 4, 2026

 Abstract

 Full text

 PDF

✓ ABSTRACT



Harnessing Built-in Polarization in a 3D/2D ZnOS/NiO-g- C_3N_4 Heterostructure for Piezo-Photocatalytic Hydrogen Evolution

K. Priyanga Kangeyan, Bernaurdshaw Neppolian, and Sandeep Kumar Lakhera*

ACS Applied Energy Materials 2026, 9, 6, 3053-3068 (Article) Subscribed

Publication Date (Web): March 2, 2026

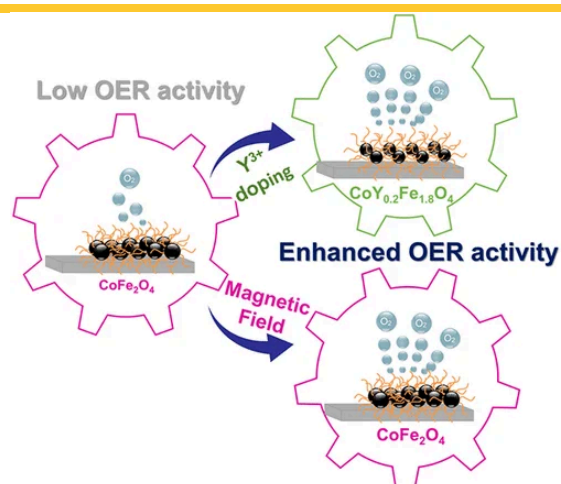
 Abstract

 Full text

 PDF

✓ ABSTRACT

ADVERTISEMENT



Magnetic-Field-Enhanced Oxygen Evolution in Yttrium-Doped CoFe_2O_4 Langmuir–Blodgett Nanofilms

Viviana Beatriz Daboin Lujano, Paula G. Bercoff*, and Julieta S. Riva*

ACS Applied Energy Materials 2026, 9, 6, 3069-3082 (Article) Subscribed

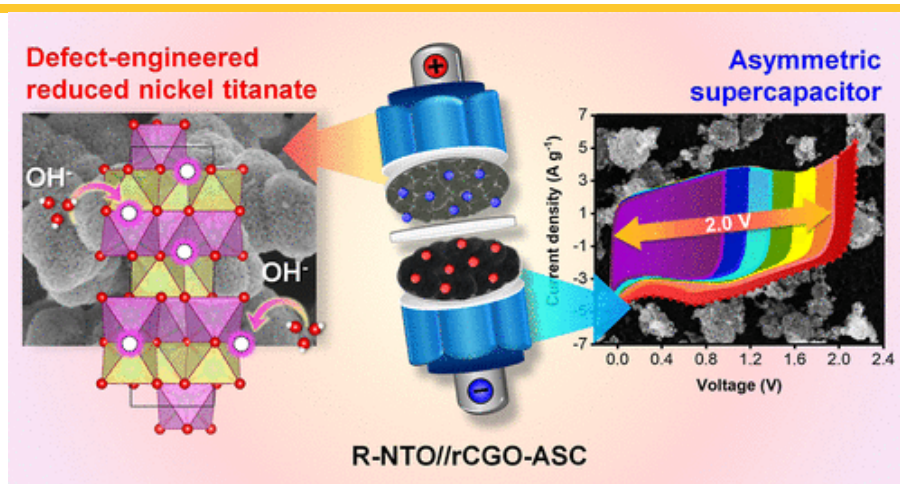
Publication Date (Web): March 9, 2026

Abstract

Full text

PDF

✓ ABSTRACT



Solid-State Defect Engineering of Nickel Titanate with Crumpled Graphene for High-Energy, Long-Life Asymmetric Supercapacitors

Nareekarn Meebua, Thanapat Jorn-am, Jedsada Manyam, Nichaphat Thongsai, Hong-Han Huang, Chun-Hu Chen*, and Peerasak Paoprasert*

ACS Applied Energy Materials 2026, 9, 6, 3083-3099 (Article) [Open Access](#)

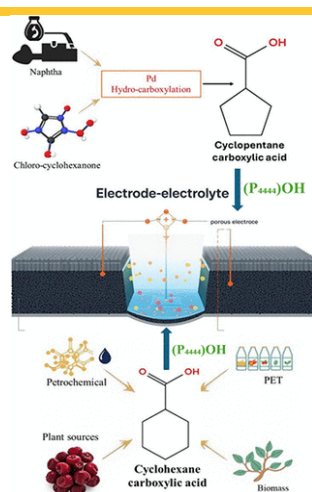
Publication Date (Web): March 10, 2026

 Abstract

 Full text

 PDF

✓ ABSTRACT



Fluorine-Free Cyclic Carboxylate Ionic Liquids as Supercapacitor Electrolyte

Gaurav Tatrari*, Sayantika Bhakta, Mukhtiar Ahmed, Solomon Tesfalidet, and Faiz Ullah Shah*

ACS Applied Energy Materials 2026, 9, 6, 3100-3115 (Article) [Open Access](#)

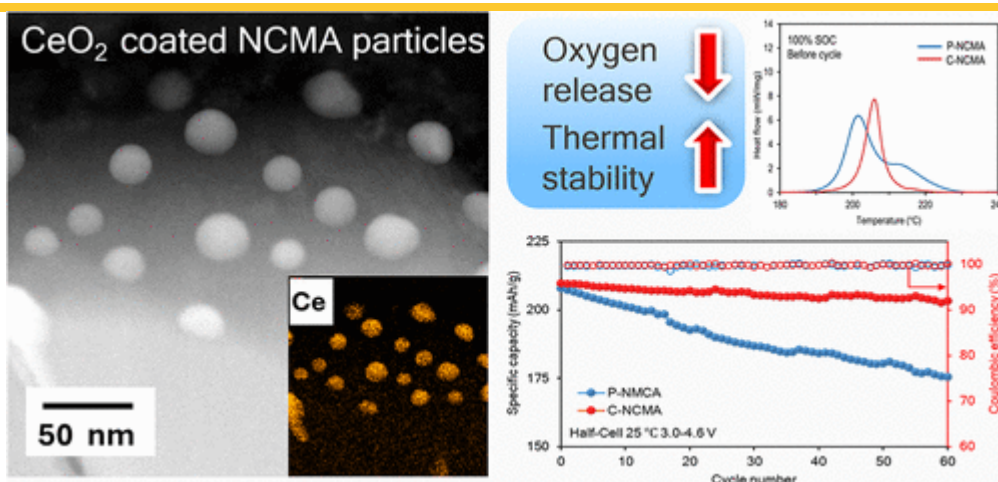
Publication Date (Web): March 4, 2026

 Abstract

 Full text

 PDF

✓ ABSTRACT



Cerium Oxide Coating on Nickel-Rich Oxide Cathodes to Mitigate Lithium-Ion Battery Thermal Runaway

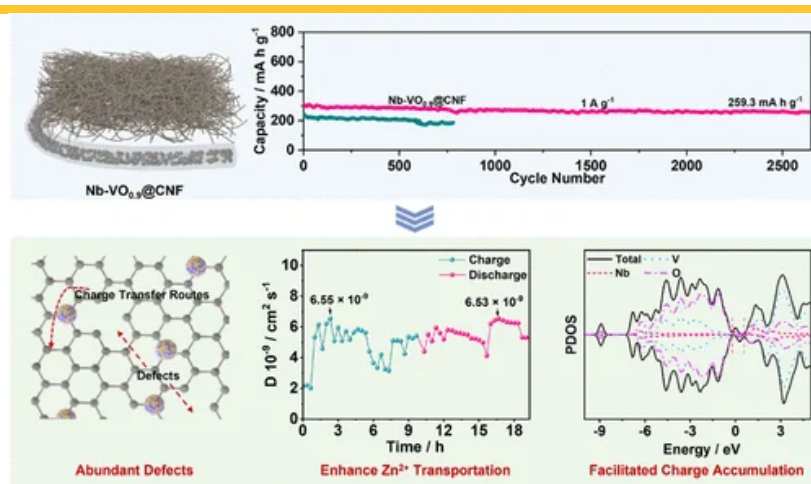
Chia-Yu Chang, Mengyuan Chen, Vamakshi Yadav, Saeed Moradi, Robert Schmidt, Lijia Liu, Jigang Zhou, Raneen Taha, Ratandeep S. Kukreja, Nicholas Paul William Pieczonka, Zhongyi Liu*, and Alan A. Luo*

ACS Applied Energy Materials 2026, 9, 6, 3116-3125 (Article) [Open Access](#)

Publication Date (Web): March 4, 2026

[Abstract](#) [Full text](#) [PDF](#)

✓ ABSTRACT



Nb-Doped VO_{0.9}@Carbon Nanofiber for High Capacitance and Fast Kinetic Zn²⁺ Ion Storage

Jinjie Huang, Yu Zhang, Maoxiang Zheng, Jianhua Zhou, Zengming Man*, Cao Wu*, Zhou Chen*, Heng Dong*, and Guan Wu

ACS Applied Energy Materials 2026, 9, 6, 3126-3133 (Article) [Subscribed](#)

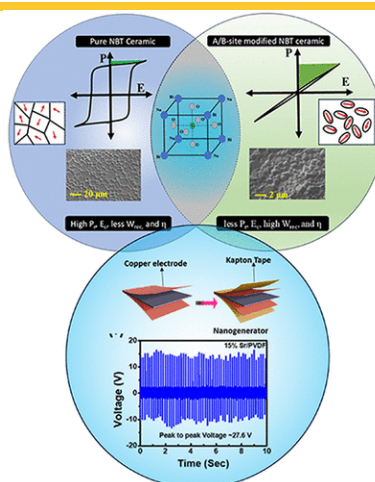
Publication Date (Web): March 9, 2026

 Abstract

 Full text

 PDF

✓ ABSTRACT



Cationic Engineering of a Sr²⁺-Modified Na_{0.5}Bi_{0.5}TiO₃-Based Ferroelectric Material for Ultra-High Energy Efficiency and Energy Harvesting

Sumit Kumar Mev, Sumit Chahal, and Saket Asthana*

ACS Applied Energy Materials 2026, 9, 6, 3134-3149 (Article) [Subscribed](#)

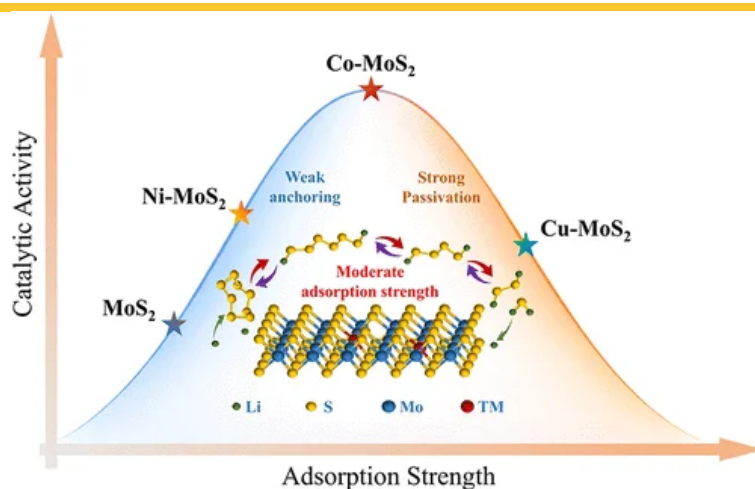
Publication Date (Web): March 2, 2026

 Abstract

 Full text

 PDF

✓ ABSTRACT



Re

Unraveling the Volcano-Type Relationship in Polysulfides Adsorption-Catalysis over MoS₂ for High-Performance Lithium–Sulfur Batteries

Hongwei Guo, Yu Yang, Xiaohui Xu, Yu Zhang, Kui Chen, Xiao-Chen Liu*, and Guangning Wu

ACS Applied Energy Materials 2026, 9, 6, 3150-3161 (Article) [Subscribed](#)

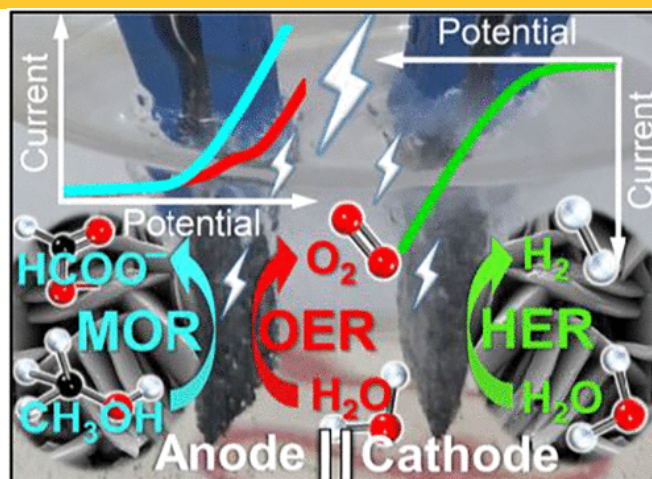
Publication Date (Web): March 5, 2026

Abstract

Full text

PDF

✓ ABSTRACT



Methanol-Assisted Hybrid Electrolysis for Green Hydrogen and Formate Production Using a Trifunctional Cu–Co–Mo Oxide Catalyst

Apurba Borah, Malaya K. Sahoo, and Gaddam Rajeshkhanna*

ACS Applied Energy Materials 2026, 9, 6, 3162-3175 (Article) Subscribed

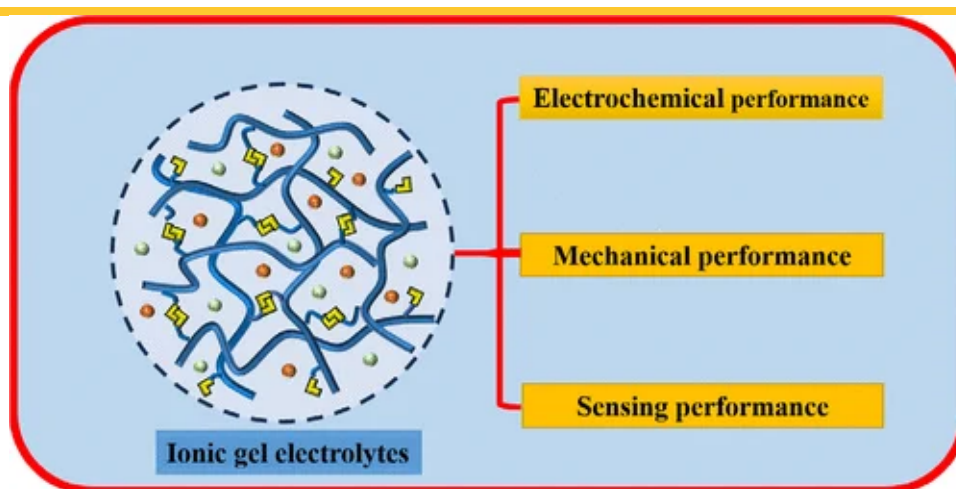
Publication Date (Web): February 26, 2026

 Abstract

 Full text

 PDF

✓ ABSTRACT



An Ether-Based Ionic Gel Electrolyte with High Ionic Conductivity and Thermal Stability Screened Based on Density Functional Theory as EDLCs

Zhixu Zhang, Xinyi Ge, Jian Wang*, Qingguo Zhang*, Ying Wei*, and Yingying Zuo*

ACS Applied Energy Materials 2026, 9, 6, 3176-3188 (Article) Subscribed

Publication Date (Web): March 11, 2026

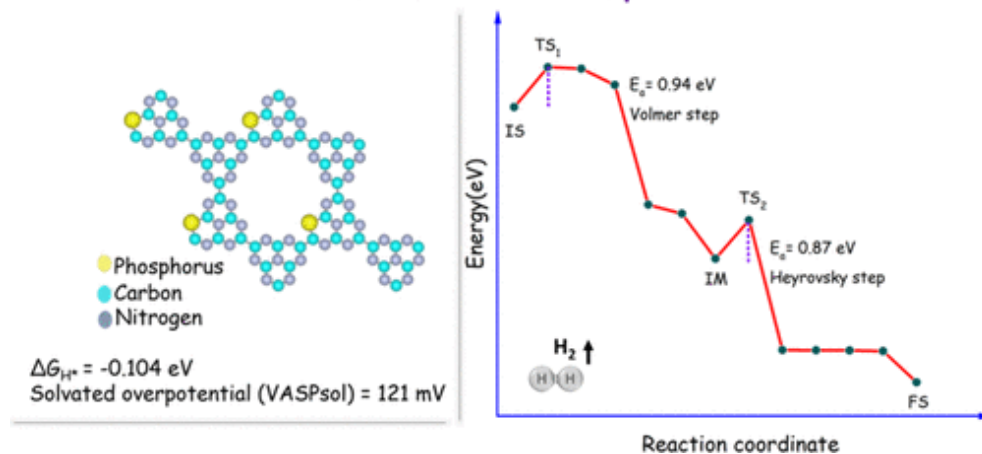
 Abstract

 Full text

 PDF

✓ ABSTRACT

Metal-Free HER Electrocatalyst



First-Principles Investigation of Phosphorus-Doped 2D C_6N_7 as a Metal-Free Electrocatalyst for the Hydrogen Evolution Reaction

Kismat K. Sahoo, J. N. Behera*, Brahmananda Chakraborty*, and Musharaf Ali Sheikh*

ACS Applied Energy Materials 2026, 9, 6, 3189-3199 (Article)

Subscribed

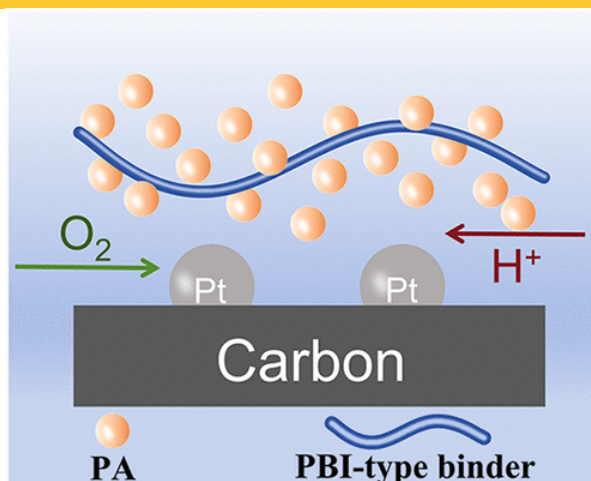
Publication Date (Web): March 6, 2026

Abstract

Full text

PDF

ABSTRACT



Optimizing Polybenzimidazole Binders for High-Temperature Proton Exchange Membrane Fuel Cells

Hong Huang, Yilin Chen, Zhihuan Pan, Jinwu Peng, Peng Wang*, and Lei Wang*

ACS Applied Energy Materials 2026, 9, 6, 3200-3209 (Article) Subscribed

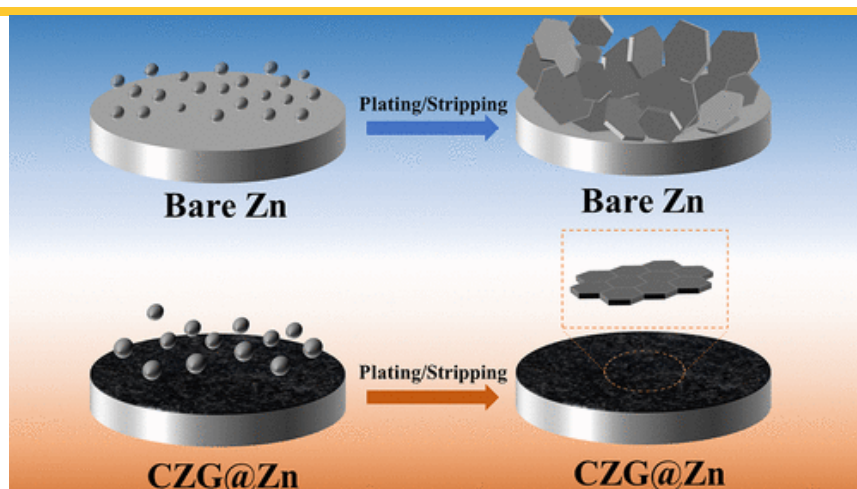
Publication Date (Web): February 27, 2026

 Abstract

 Full text

 PDF

✓ ABSTRACT



Constructing a Hybrid Cu-ZIF/rGO Artificial Protective Layer toward Stable Dendrite-Free Zinc Anodes in Aqueous Zinc-Ion Batteries

Jinkai Zhang, Lirong Feng, Xinru Zheng, Jiangyan Xie, and Xiaohui Guo*

ACS Applied Energy Materials 2026, 9, 6, 3210-3218 (Article) Subscribed

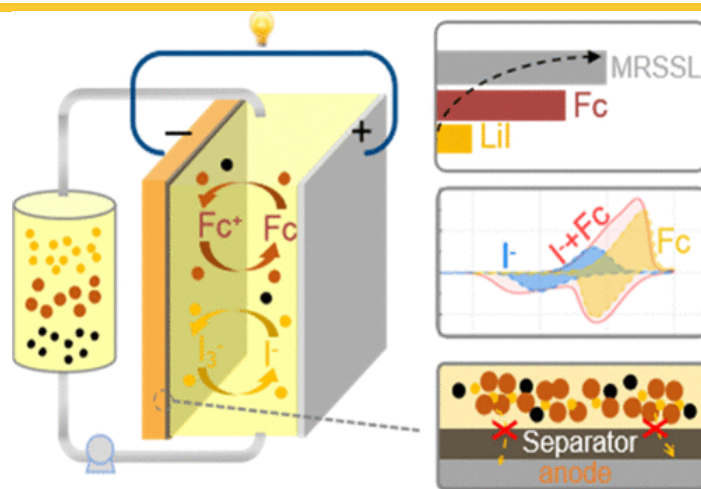
Publication Date (Web): March 11, 2026

 Abstract

 Full text

 PDF

✓ ABSTRACT



Re

A High-Efficiency Iodide-Ferrocene Multiple Redox Suspension for Li-Based Flow Batteries

Yunzhan Liu, Xuefeng Zhang, and Hongning Chen*

ACS Applied Energy Materials 2026, 9, 6, 3219-3226 (Article) [Subscribed](#)

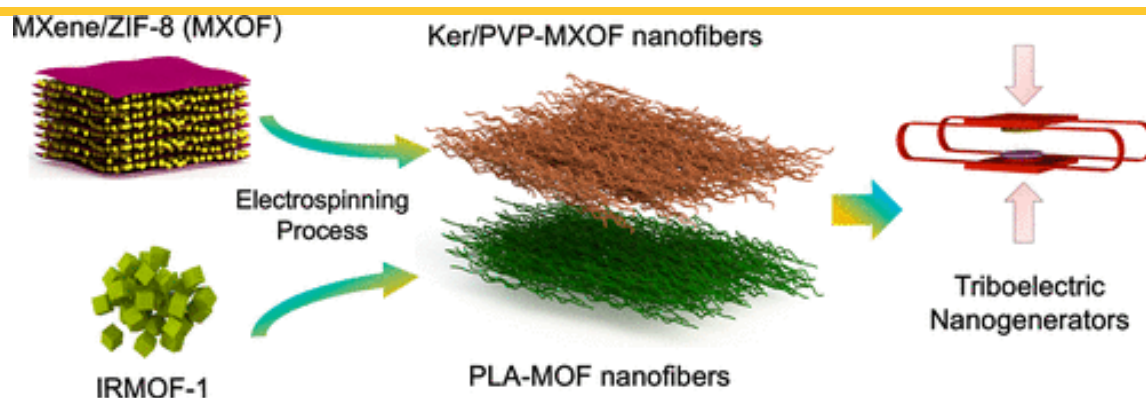
Publication Date (Web): March 11, 2026

Abstract

Full text

PDF

✓ ABSTRACT



Flexible Triboelectric Nanogenerators Based on Nanofibrous Membranes Integrated with MOF and MXene/MOF Composites

Ömer Faruk Ünsal, Mahdi Hasanzadeh*, and Ayse Celik Bedeloglu

ACS Applied Energy Materials 2026, 9, 6, 3227-3239 (Article) [Subscribed](#)

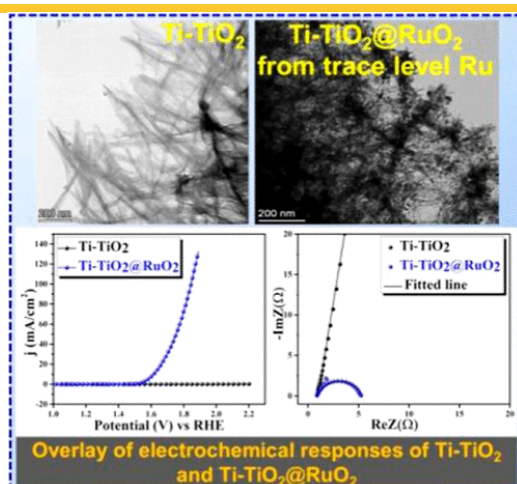
Publication Date (Web): February 27, 2026

Abstract

Full text

PDF

✓ ABSTRACT



Mixed Metal Oxide $\text{TiO}_2\text{@RuO}_2$ Nanostructure over Titanium Substrates as Self-Supporting Electrodes for Oxygen Evolution Reaction

A. G. Kamaha Tchekep, S. Devaraj, V. Suryanarayanan, and Deepak K. Pattanayak*

ACS Applied Energy Materials 2026, 9, 6, 3240-3252 (Article) [Subscribed](#)

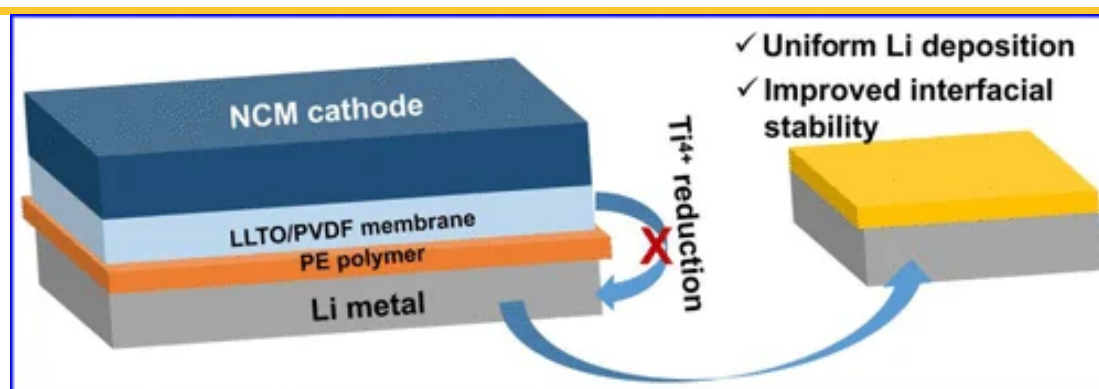
Publication Date (Web): March 11, 2026

[Abstract](#)

[Full text](#)

[PDF](#)

✓ ABSTRACT



Interface-Stabilized LLTO/PVDF/PE Composite Separator Boosts High-Performance All-Solid-State Lithium Metal Batteries

Wenxin Shi, Qingmei Su*, Xuan Li, Huayu Li, Siyu Wang, Weihao Shi, Liming Wang, Yinyin Song, Shan Yang, Gaohui Du*, Miao Zhang, Wenqi Zhao, and Bingshe Xu

ACS Applied Energy Materials 2026, 9, 6, 3253-3262 (Article) [Subscribed](#)

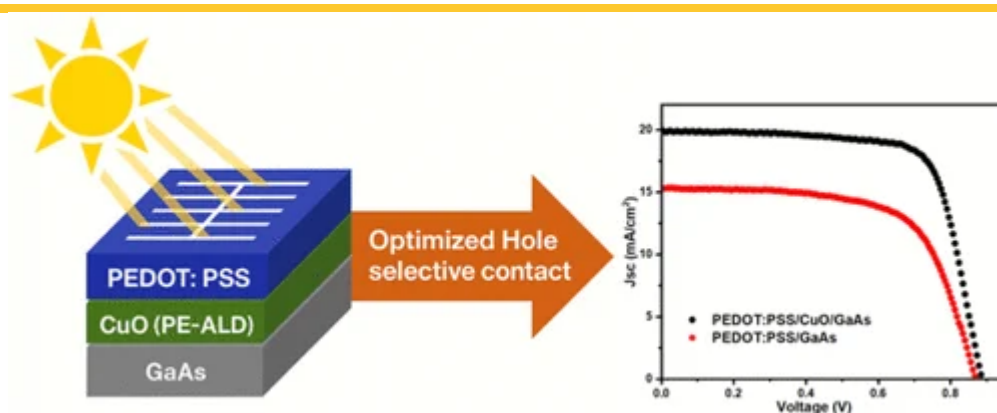
Publication Date (Web): March 6, 2026

 Abstract

 Full text

 PDF

✓ ABSTRACT



Ultrathin CuO Hole-Selective Contact for Efficient GaAs Solar Cells

Parul Duhan*, Gabriel Bartholazzi, Tuomas Haggren, Bikesh Gupta, Sonachand Adhikari, Lachlan E. Black, Doudou Zhang, Chennupati Jagadish, Siva Karuturi, and Hark Hoe Tan*

ACS Applied Energy Materials 2026, 9, 6, 3263-3271 (Article) [Subscribed](#)

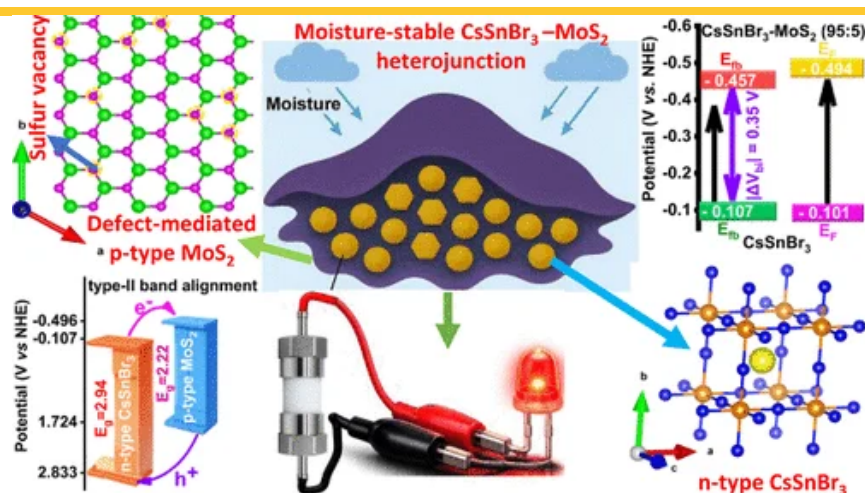
Publication Date (Web): March 9, 2026

 Abstract

 Full text

 PDF

✓ ABSTRACT



Interfacial Engineering of Moisture-Stable CsSnBr₃-MoS₂ Heterostructures for High-Voltage Aqueous Energy Storage

Mohasin Tarek and M. A. Basith*

ACS Applied Energy Materials 2026, 9, 6, 3272-3284 (Article) [Subscribed](#)

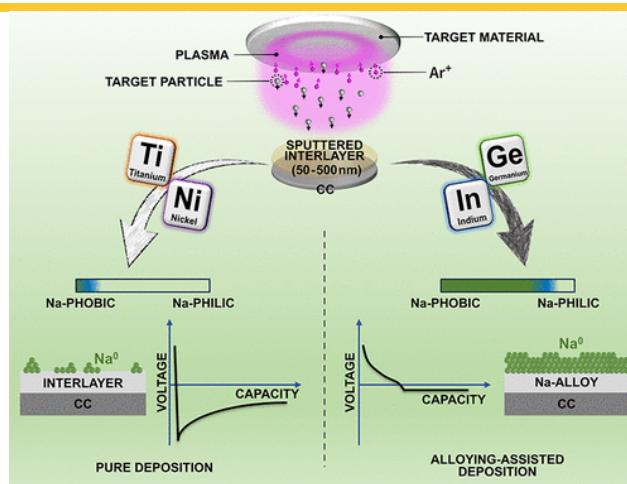
Publication Date (Web): March 4, 2026

[Abstract](#)

[Full text](#)

[PDF](#)

✓ ABSTRACT



Thickness-Dependent Engineering of Sodiophilic Sputtered (In, Ge, Ti, Ni) Interlayers for Anode-Free Sodium Batteries

Lorenzo Fallarino*, Mert Yalçınöz, Miren De Lasen, Yan Zhang, and Rosalia Cid*

ACS Applied Energy Materials 2026, 9, 6, 3285-3300 (Article) Subscribed

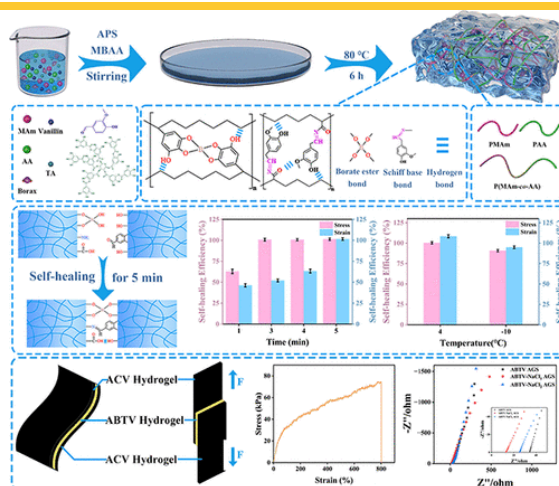
Publication Date (Web): March 9, 2026

 Abstract

 Full text

 PDF

✓ ABSTRACT



Self-Healing Hydrogels with Triple Dynamic Bond Synergy for All-Gel Supercapacitors

Zichun Zhao, Yihan Guo, Xin Guan, Honglei Liu, Wenjun Kang, Yongqi Yang, Hailun Ren, Jian Sun, Zhaohui Jin, and Zijian Gao*

ACS Applied Energy Materials 2026, 9, 6, 3301-3313 (Article) Subscribed

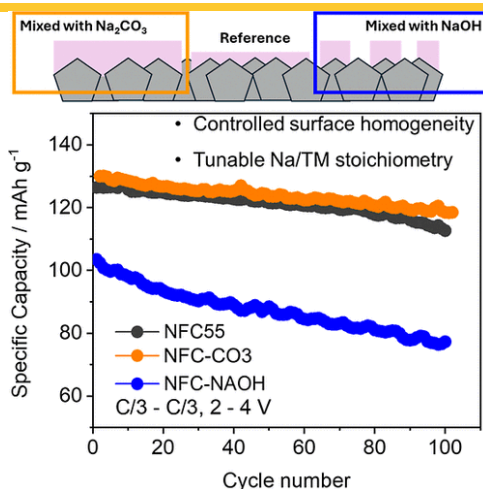
Publication Date (Web): March 4, 2026

 Abstract

 Full text

 PDF

✓ ABSTRACT



Re

Tuning Sodium Source Chemistry for Enhanced Structural Homogeneity and Kinetic Properties of Sol–Gel Layered Cathode in Sodium-Ion Batteries

Hoang Van Nguyen*, Minh Le Nguyen, Phung My Loan Le, and Van Man Tran

ACS Applied Energy Materials 2026, 9, 6, 3314-3327 (Article) [Subscribed](#)

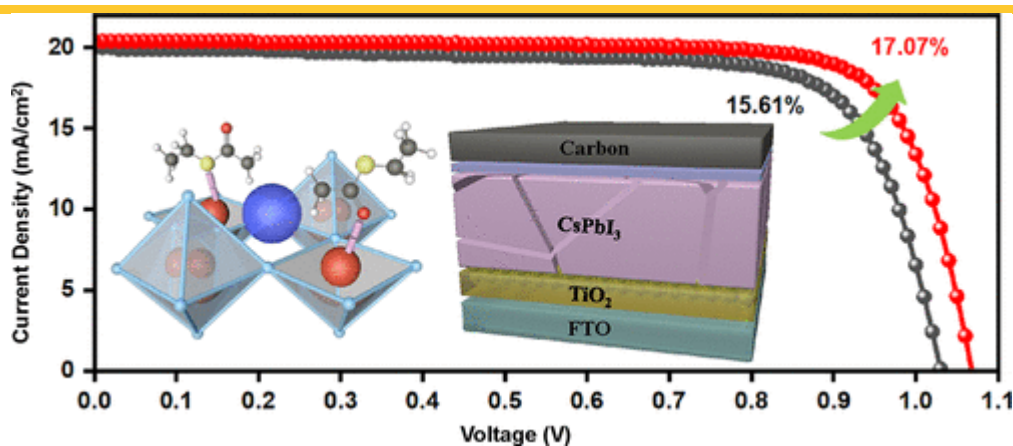
Publication Date (Web): February 28, 2026

[Abstract](#)

[Full text](#)

[PDF](#)

✓ ABSTRACT



Facile Molecular Modification for Efficient and Stable Carbon-Based CsPbI₃ Perovskite Solar Cells

Zhixing Wang, Jinqing Lv, Weifeng Liu, Weiwei Sun, Zhiwen Dong, Kexiang Wang, Tingting You*, and Penggan Yin*

ACS Applied Energy Materials 2026, 9, 6, 3328-3336 (Article) [Subscribed](#)

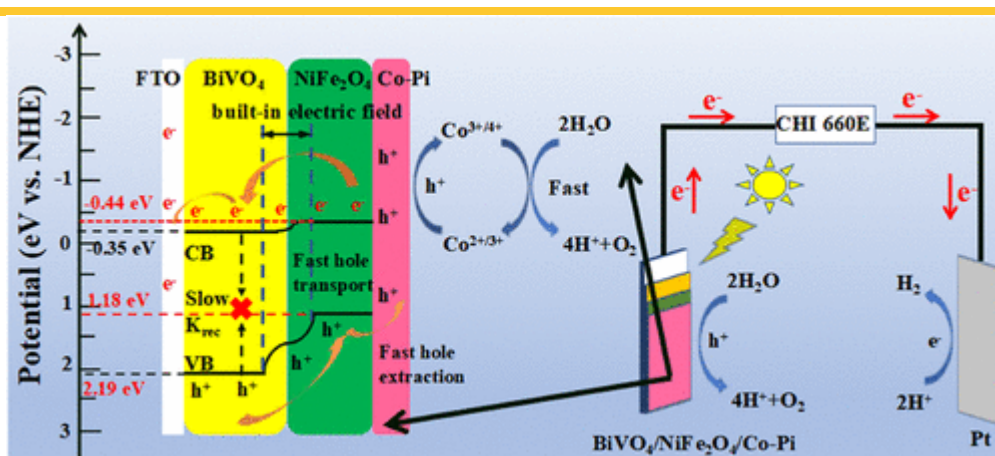
Publication Date (Web): March 9, 2026

[Abstract](#)

[Full text](#)

[PDF](#)

ABSTRACT



Rational Design of Ternary BiVO₄/NiFe₂O₄/Co-Pi Photoanodes with Hole Transport and Extraction Units for Enhanced Photoelectrochemical Water Splitting

Zemin Fu, Xu Niu, Bowen Zhang, Chuangshi Liu, Sheng Han, and Zhenbiao Dong*

ACS Applied Energy Materials 2026, 9, 6, 3337-3349 (Article) [Subscribed](#)

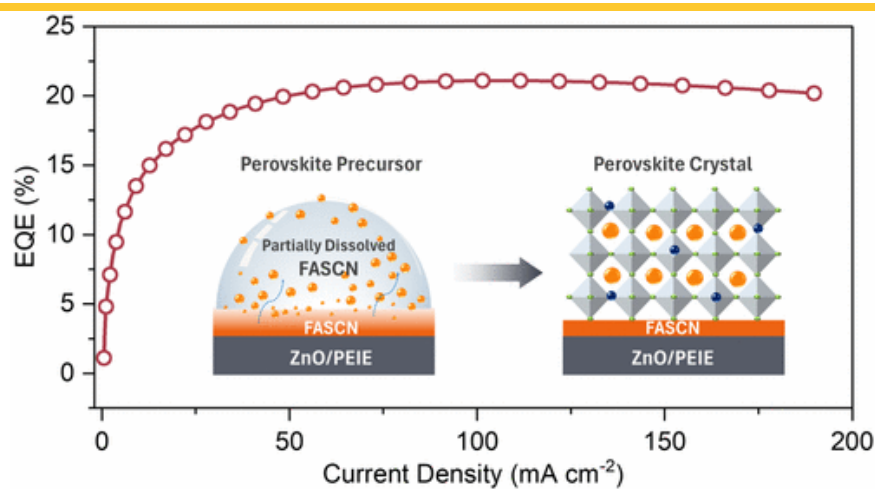
Publication Date (Web): March 3, 2026

[Abstract](#)

[Full text](#)

[PDF](#)

ABSTRACT



Synergistic Interface–Bulk Passivation Induced by a Pre-Additive Modifier for Efficient Near-Infrared Perovskite Light-Emitting Diodes

Xin-Yuan Gao, Xin-Ye Wu, Wei-Zhi Liu, Shuai-Hao Xu, Dong-Ying Zhou*, and Liang-Sheng Liao*

ACS Applied Energy Materials 2026, 9, 6, 3350-3359 (Article) Subscribed

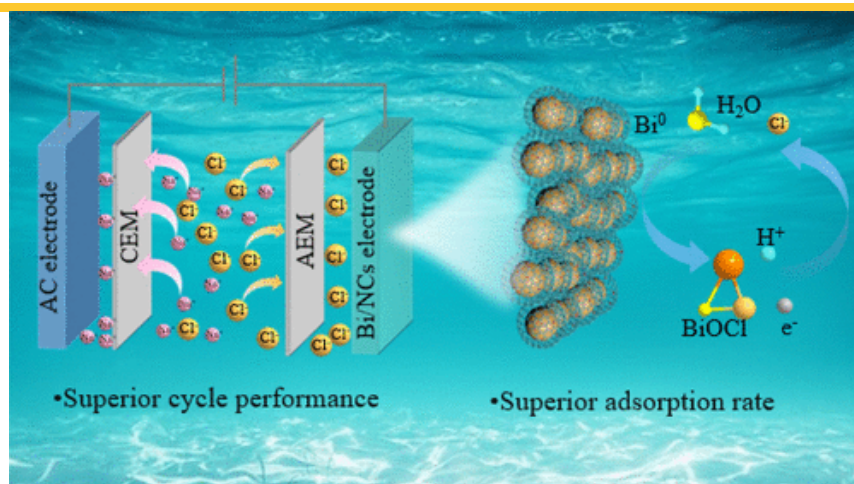
Publication Date (Web): March 11, 2026

Abstract

Full text

PDF

▼ ABSTRACT



Bismuth Nanoparticles Encapsulated in Nitrogen-Doped Carbon Hierarchical Porous Spheres as a Chloride Ion Capturing Electrode for Capacitive Deionization

Nan A, Qingtao Ma*, Wanxia Luo*, Dianzeng Jia, Nannan Guo, Mengjiao Xu, Lili Ai, Changyu Leng, and Luxiang Wang* Re

ACS Applied Energy Materials 2026, 9, 6, 3360-3371 (Article) Subscribed

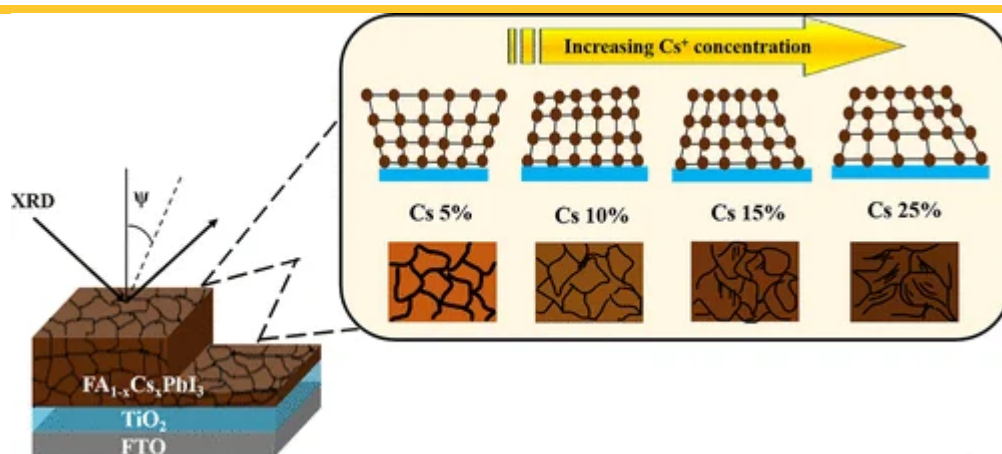
Publication Date (Web): March 4, 2026

 Abstract

 Full text

 PDF

✓ ABSTRACT



Performance Optimization of Air-Processed Perovskite Solar Cells via Compositional Engineering and Residual Stress Analysis

Mrittika Paul*, Sutapa Dey, and Trilok Singh*

ACS Applied Energy Materials 2026, 9, 6, 3372-3385 (Article) Subscribed

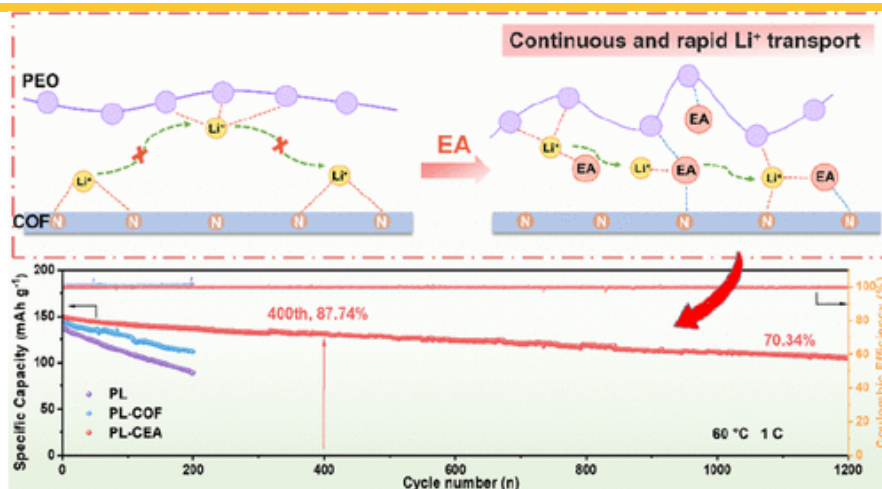
Publication Date (Web): March 2, 2026

 Abstract

 Full text

 PDF

✓ ABSTRACT



Efficient Shuttling of Li^+ by an Amide at the COF/PEO Interface in a Composite Solid Polymer Electrolyte

Yaping Sun, Bing Li, Jing Li, Yimei Jin, Cheng Lian, Honglai Liu, Jingkun Li*, and Haiping Su*

ACS Applied Energy Materials 2026, 9, 6, 3386-3393 (Article) [Subscribed](#)

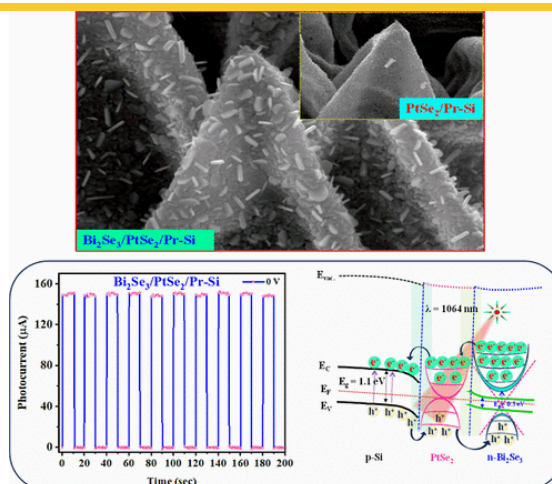
Publication Date (Web): March 5, 2026

[Abstract](#)

[Full text](#)

[PDF](#)

ABSTRACT



A Multi-Interface Engineered Bi₂Se₃/PtSe₂ Heterojunction on Pyramid Si Nanostructures for Self-Powered Near-Infrared Photodetection

Rahul Kumar, Bheem Singh, Aditya Yadav, Ruchi K. Sharma, Ramakrishnan Ganesan, Sanjay K. Srivastava, Senthil Kumar Muthusamy, Govind Gupta, and Sunil Singh Kushvaha*

ACS Applied Energy Materials 2026, 9, 6, 3394-3404 (Article) [Subscribed](#)

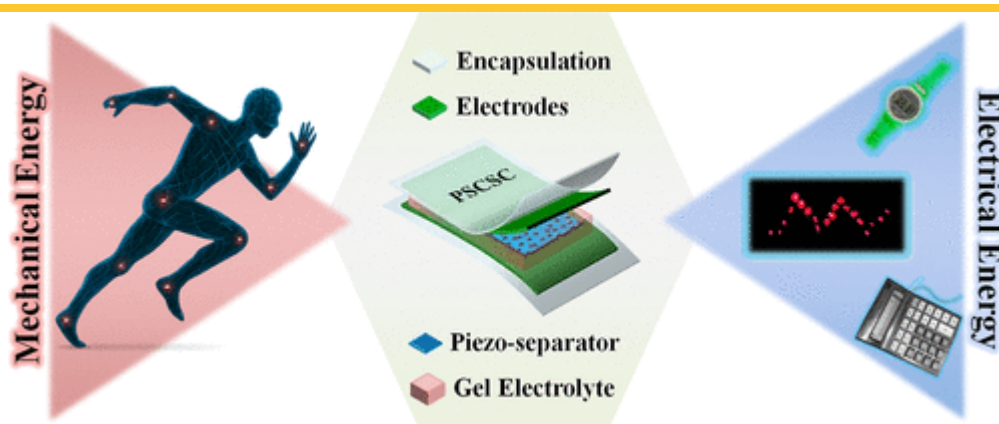
Publication Date (Web): March 2, 2026

 Abstract

 Full text

 PDF

▼ ABSTRACT



Design of a β -Phase-Stabilized High-Performance Porous PVDF/BaSnO₃-rG Piezoelectric Nanogenerator Film and Its Integration into a Piezo-Driven Self-Charging Supercapacitor

Sumanta Bera, Parna Maity, Nil Lohit Sengupta, Suparna Ojha, and Bhanu Bhusan Khatua*

ACS Applied Energy Materials 2026, 9, 6, 3405-3418 (Article) [Subscribed](#)

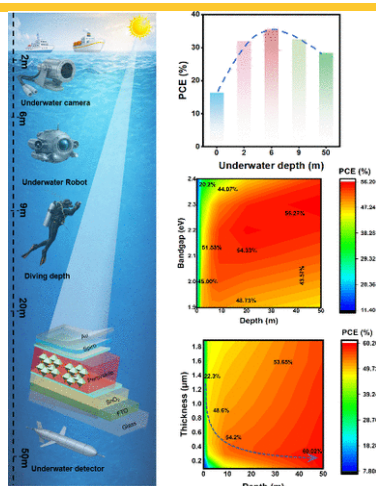
Publication Date (Web): March 3, 2026

 Abstract

 Full text

 PDF

▼ ABSTRACT



Re

Theoretical Insights into Depth-Adaptive Bandgap Engineering Enabling Over-60%-Efficient Perovskite Photovoltaics in Deep-Sea Environments

Yu Cao, Zhihui Han, Sanlong Wang, Zhenwang Luo, Xiaohui Liu, Ziyang Hu*, Qi Liu, and Jing Zhou*

ACS Applied Energy Materials 2026, 9, 6, 3419-3431 (Article) [Subscribed](#)

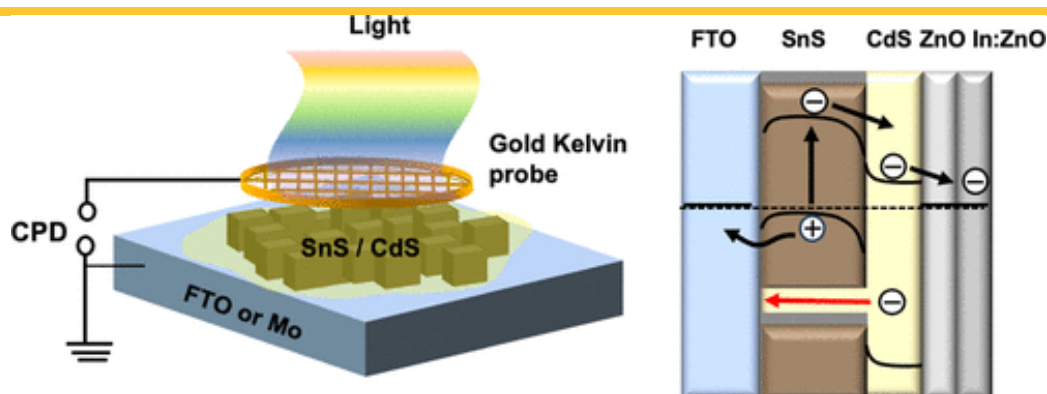
Publication Date (Web): March 3, 2026

[Abstract](#)

[Full text](#)

[PDF](#)

✓ ABSTRACT



Understanding Photovoltage Deficits in Electrochemically Grown Tin Sulfide (SnS) Thin-Film Photovoltaic Devices

Zainab Najaf, Jade Paranhos Lopes, Nicolas Gaillard, Moisés A. de Araújo, Mahya Salmanion, Rajesh Kandel, Wang, and Frank E. Osterloh*

ACS Applied Energy Materials 2026, 9, 6, 3432-3442 (Article) [Subscribed](#)

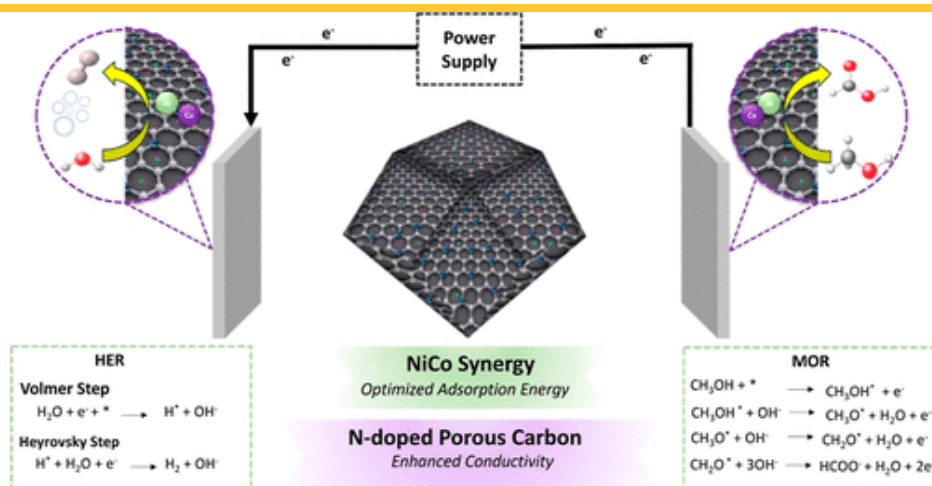
Publication Date (Web): March 10, 2026

[Abstract](#)

[Full text](#)

[PDF](#)

✓ ABSTRACT



ZIF-8-Derived Dodecahedral NiCo Nanostructure for Energy-Efficient Methanol-Assisted Seawater Electrolysis

Faiza Zulfiqar*, Irfan Ullah, Amna Zahid, M. A. Rafiq, and Falak Sher*

ACS Applied Energy Materials 2026, 9, 6, 3443-3454 (Article) [Subscribed](#)

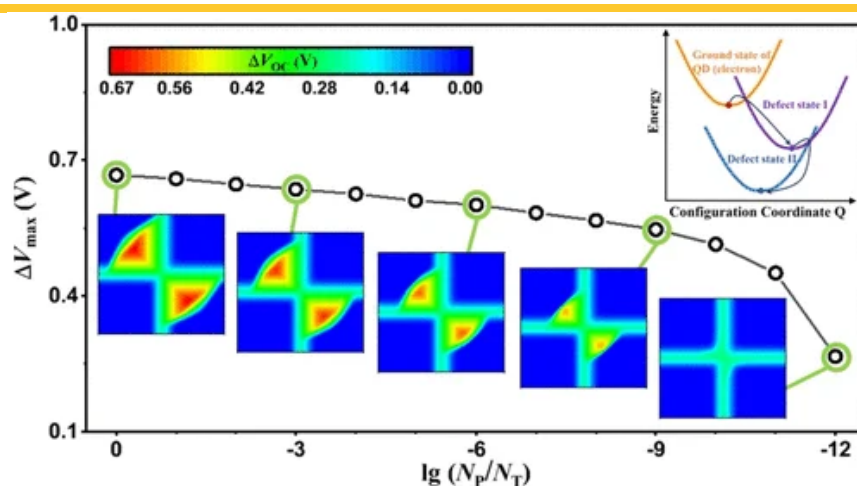
Publication Date (Web): March 9, 2026

[Abstract](#)

[Full text](#)

[PDF](#)

ABSTRACT



Maps for Open-Circuit Voltage Losses Caused by Defects in Metal Halide Perovskite Quantum Dot Solar Cells

Ran-Bo Yang, Xiao-Qi Dong, Ming-Hao Li, Yue-Wen Wang, Zhi-Qing Li, Li-Xia Zhao, and Zi-Wu Wang*

ACS Applied Energy Materials 2026, 9, 6, 3455-3461 (Article) [Subscribed](#)

Publication Date (Web): March 11, 2026

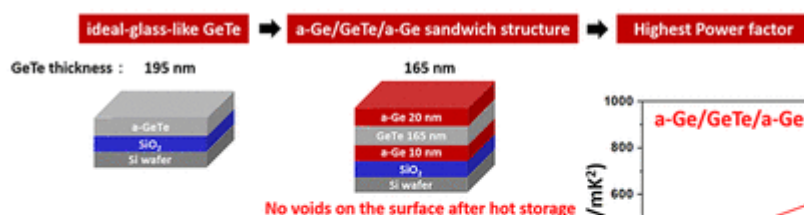
 Abstract

 Full text

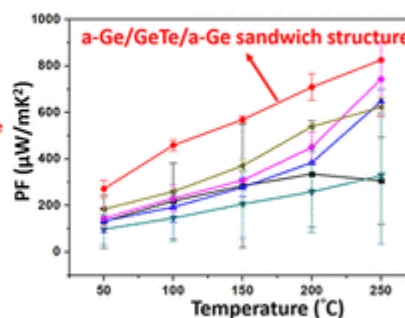
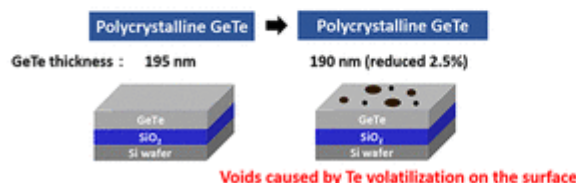
 PDF

✓ ABSTRACT

■ Schematic of **ideal-glass-like GeTe** undergoing 30 days of hot storage at 350 °C



■ Schematic of **crystalline GeTe** undergoing 30 days of hot storage at 350 °C



Decisive Role of Initial Crystallinity in Spontaneously Forming High-Performance a-Ge/GeTe/a-Ge Sandwich Thermoelectric Films

Chun-Yung Huang, Chun-Han Ku, Cheng-Yen Yang, V. K. Ranganayakulu, Yang-Yuan Chen, Yan-Gu Lin, Shang-Chiu, Chia-Jung Hsu, and Albert T. Wu*

ACS Applied Energy Materials 2026, 9, 6, 3462-3471 (Article) [Open Access](#)

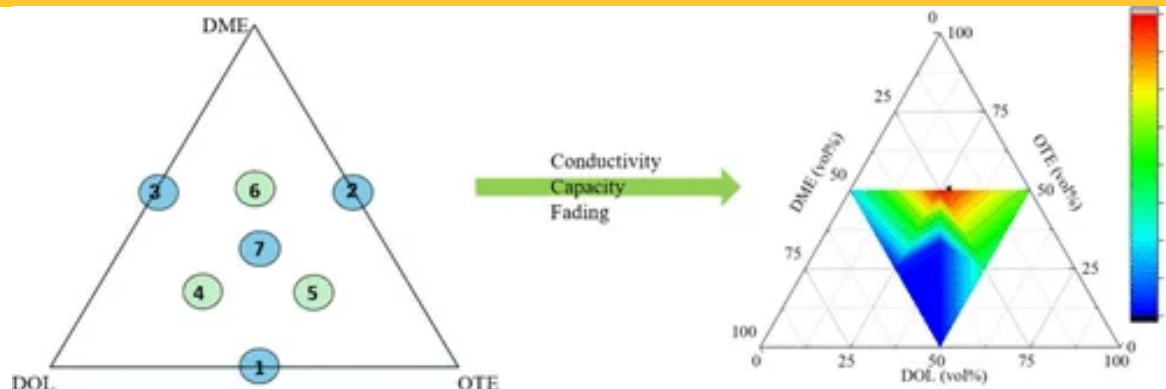
Publication Date (Web): March 4, 2026

 Abstract

 Full text

 PDF

✓ ABSTRACT



Re

Optimization of Fluorinated Ether-Based Quasi-Solid Electrolyte Systems for Lithium–Sulfur Batteries

Ishani Senevirathna*, Changlong Chen, Junquan Ou, Vignyaatha Tatagari, Leon Shaw, and Carlo U. Segre

ACS Applied Energy Materials 2026, 9, 6, 3472-3483 (Article) [Open Access](#)

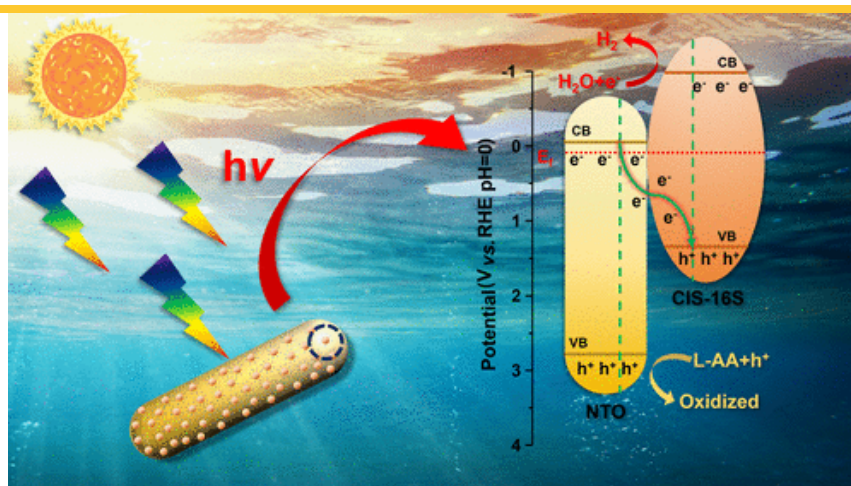
Publication Date (Web): March 11, 2026

Abstract

Full text

PDF

✓ ABSTRACT



Nonstoichiometric Sulfur Engineering in a 3D/0D NiTiO₃/CuIn₅S₈ Heterojunction for Enhanced Photocatalytic Hydrogen Evolution

Pengfei Zhou, Mingqiang Fan, Cheng Ye, Tao Wang, Bo Yang, Miaolian Ma, Wanpeng Zhou, Ling Qin, Bin Li, Chuanliang Wei, Jie Ren*, and Maofeng Zhang*

ACS Applied Energy Materials 2026, 9, 6, 3484-3496 (Article) [Subscribed](#)

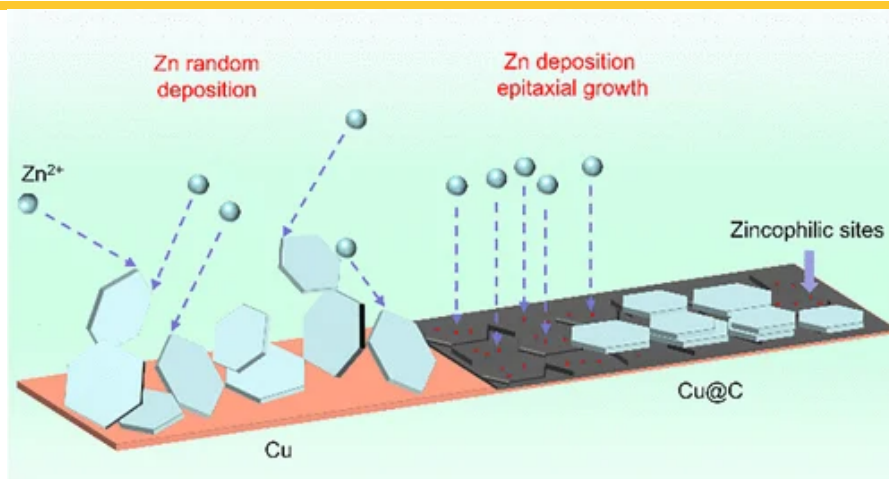
Publication Date (Web): March 9, 2026

Abstract

Full text

PDF

✓ ABSTRACT



Functionalized Graphite Nanosheet Interfaces Enable (002)-Oriented Epitaxial Zinc Growth in Aqueous Zinc-Ion Batteries

Wei Weng, Jiehong Liu, Shuiping Zhong, Jiaozhong Cai, Guangsheng Zeng, Junnan Chen, Xiaopeng Chi, and Wen Tan*

ACS Applied Energy Materials 2026, 9, 6, 3497-3505 (Article) [Subscribed](#)

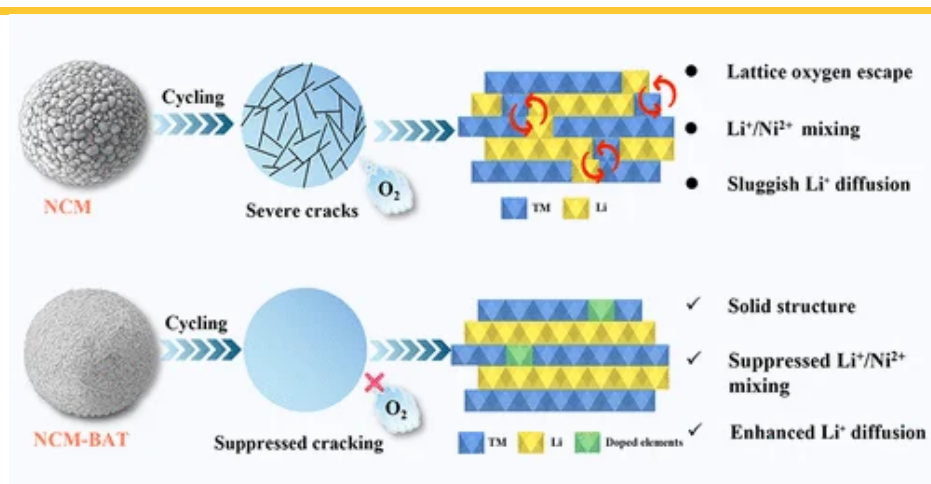
Publication Date (Web): March 2, 2026

Abstract

Full text

PDF

✓ ABSTRACT



Multi-Element Synergistic Doping Enables Cooperative Structural Stabilization of Ultra-High-Nickel Cathodes

Caiyan Qiu, Huazhang Zhou, Mingle Chu, Peng Gao, Xudong Li*, and Yongming Zhu*

ACS Applied Energy Materials 2026, 9, 6, 3506-3516 (Article) [Subscribed](#)

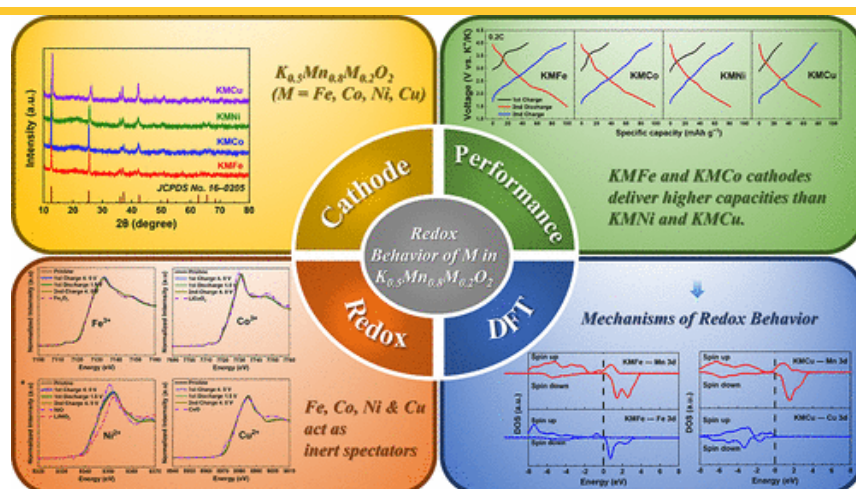
Publication Date (Web): March 11, 2026

 Abstract

 Full text

 PDF

✓ ABSTRACT



Unexpected Redox-Inert Behaviors and Their Mechanisms of Doped Transition Metals in $K_{0.5}MnO_2$ Cathodes

Cheng Zhang, Rui-Jie Luo, Chong-Yu Du, Jie Zeng, Zhe Qian, Zhe Mei, Zi-Ting Zhou, Le Yu*, and Yong-Ning Zhou*

ACS Applied Energy Materials 2026, 9, 6, 3517-3524 (Article) [Subscribed](#)

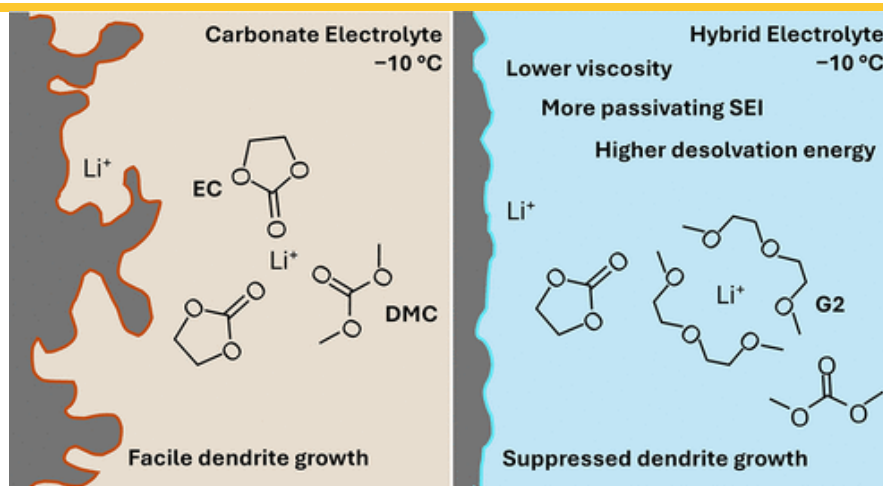
Publication Date (Web): February 27, 2026

 Abstract

 Full text

 PDF

✓ ABSTRACT



Re

Impact of Diglyme Cosolvent on Low-Temperature Microstructural Lithium Growth

Olivia A. Wander, Anaya Khan, Euan N. Bassey, Tyler Pennebaker, Harrison Szeto, Leo W. Gordon, Neva Luthria Oscar A. Nordness, Yangying Zhu*, and Raphaële J. Clément*

ACS Applied Energy Materials 2026, 9, 6, 3525-3537 (Article) [Subscribed](#)

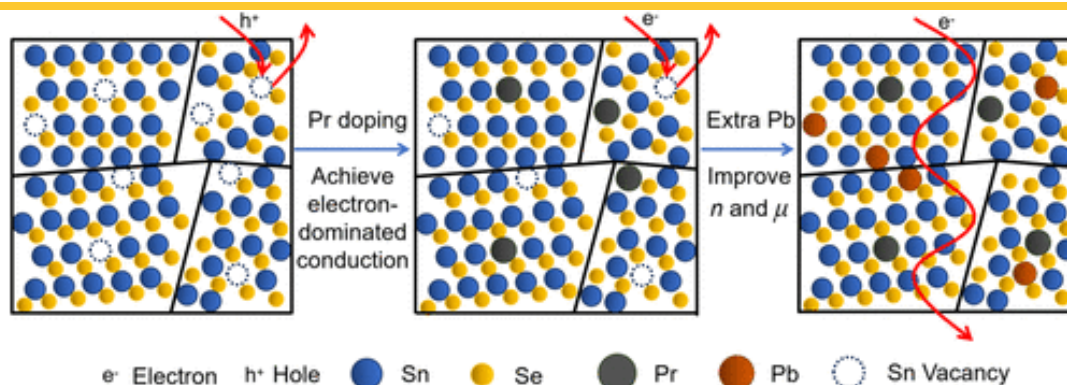
Publication Date (Web): March 11, 2026

[Abstract](#)

[Full text](#)

[PDF](#)

✓ ABSTRACT



Enhancing Thermoelectric Performance of n-Type SnSe Polycrystals through Rare-Earth Element Doping and Vacancy Compensation

Minghao Yuan, Xumeng Jia, Shulin Bai, Yixuan Hu, Yulong Gao, Changzhen Zhang, Lei Wang, Tian Gao, Baocheng Yuan, Lizhong Su, Cheng Chang*, and Li-Dong Zhao*

ACS Applied Energy Materials 2026, 9, 6, 3538-3544 (Article) [Subscribed](#)

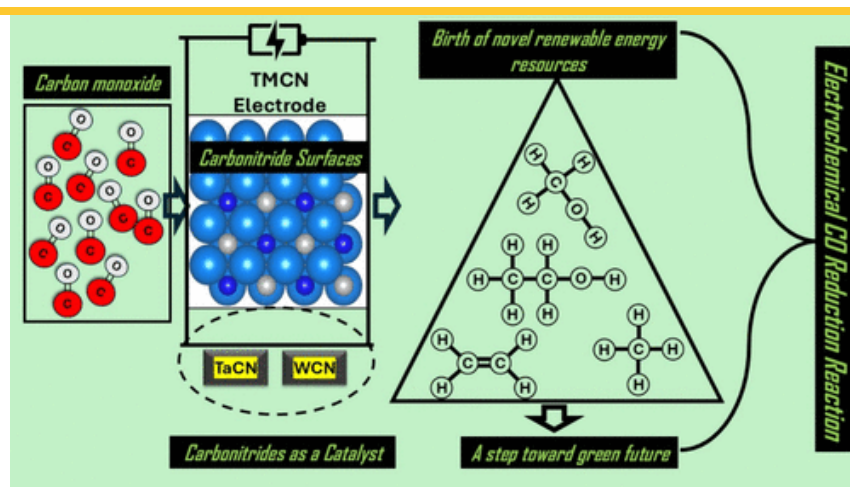
Publication Date (Web): March 6, 2026

 Abstract

 Full text

 PDF

✓ ABSTRACT



Surface Coverage-Controlled C–C Coupling for Sustainable Formation of C1 and C2 Products

Muhammad Awais* and Younes Abghoui*

ACS Applied Energy Materials 2026, 9, 6, 3545-3555 (Article) [Subscribed](#)

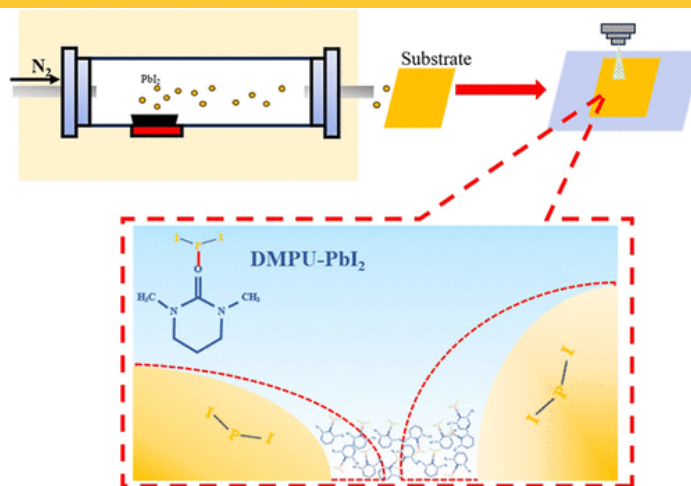
Publication Date (Web): March 3, 2026

 Abstract

 Full text

 PDF

✓ ABSTRACT



Re

Gap-Filling and Crystallization Kinetics Regulation in VTD/Spray Hybrid Perovskite Solar Cells

Kun Yu, Tian Zhong, JiaWei Zhang, Lu Zhang, Bin Li, and Yong Peng*

ACS Applied Energy Materials 2026, 9, 6, 3556-3564 (Article) [Subscribed](#)

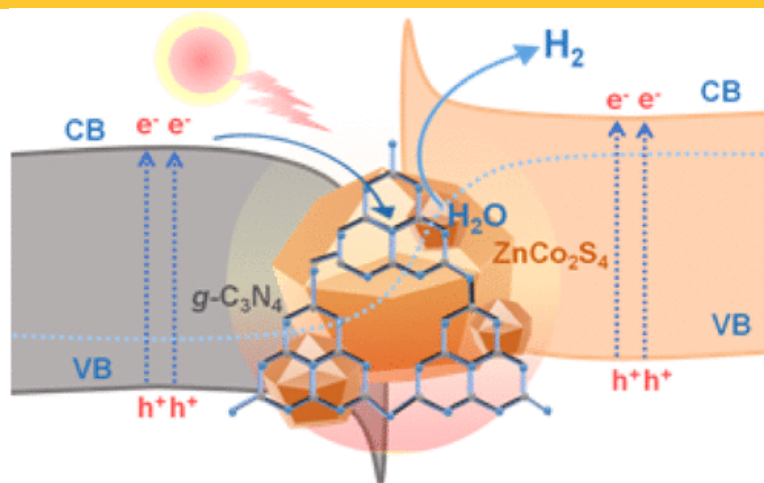
Publication Date (Web): March 3, 2026

Abstract

Full text

PDF

✓ ABSTRACT



Modulation of Sulfur Vacancies in MOF-Derived 3D Hollow ZnCo₂S₄ Polyhedra on 2D g-C₃N₄ Nanosheets for Enhanced Photocatalytic Hydrogen Evolution

Hafijul Islam, Asif Iqbal, Bhavya Jaksani, Switi Dattatraya Kshirsagar, Kathi Sudarshan, Ranjit Thapa, Mohsen Ahmadipour, and Ujjwal Pal*

ACS Applied Energy Materials 2026, 9, 6, 3565-3576 (Article) Subscribed

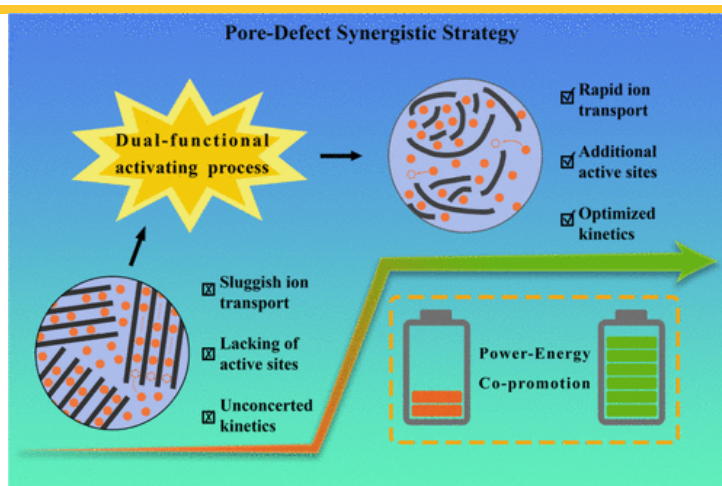
Publication Date (Web): March 5, 2026

 Abstract

 Full text

 PDF

✓ ABSTRACT



Optimal Kinetics Carbon Anodes via Dual-Functional Activation of Pores and Defects for Lithium-Ion Capacitors

Huize Zhang, Dong Shi, Yang Xu, Mingzhi Yang, Zizheng Ai, Yongliang Shao, Yongzhong Wu*, and Xiaopeng Hao*

ACS Applied Energy Materials 2026, 9, 6, 3577-3585 (Article) Subscribed

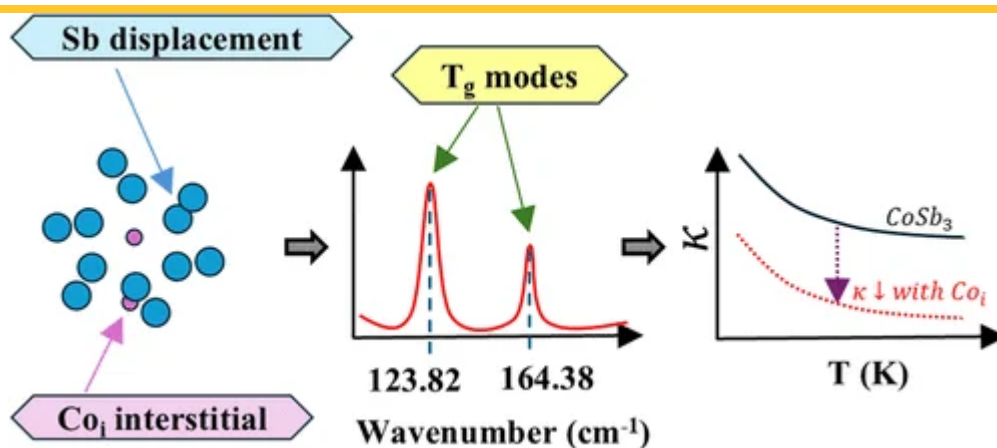
Publication Date (Web): March 7, 2026

 Abstract

 Full text

 PDF

✓ ABSTRACT



Re

Exploring the Role of Interstitial Occupation of Cobalt on the Thermoelectric Properties of Co-Excess Te-Substituted Skutterudite CoSb₃

Saagar Devassy Chaklathy, Tanu Choudhary, Gowtham Venkatesan, Satyam Suwas, Raju K. Biswas, and Ramesh Chandra Mallik*

ACS Applied Energy Materials 2026, 9, 6, 3586-3600 (Article) [Subscribed](#)

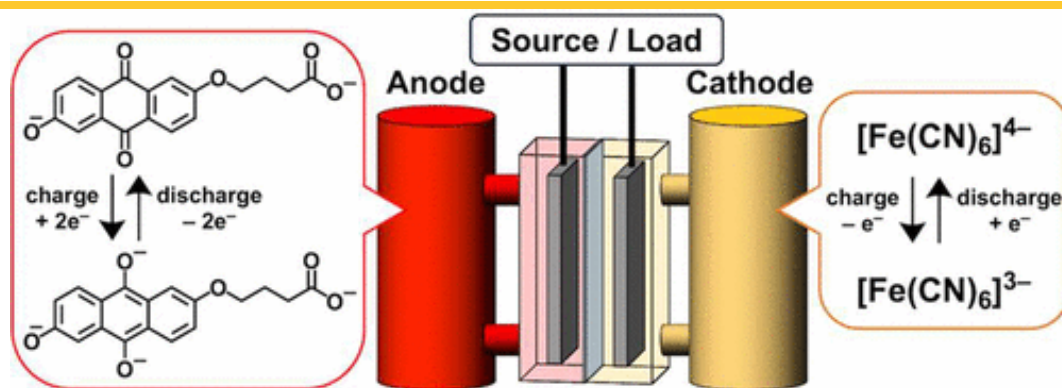
Publication Date (Web): March 11, 2026

[Abstract](#)

[Full text](#)

[PDF](#)

ABSTRACT



A Highly Stable and Soluble Asymmetric Anthraquinone Derivative for Aqueous Redox Flow Batteries

Tsuyoshi Murata*, Aya Ito, Shigemitsu Okada, and Yasushi Morita*

ACS Applied Energy Materials 2026, 9, 6, 3601-3607 (Article) [Subscribed](#)

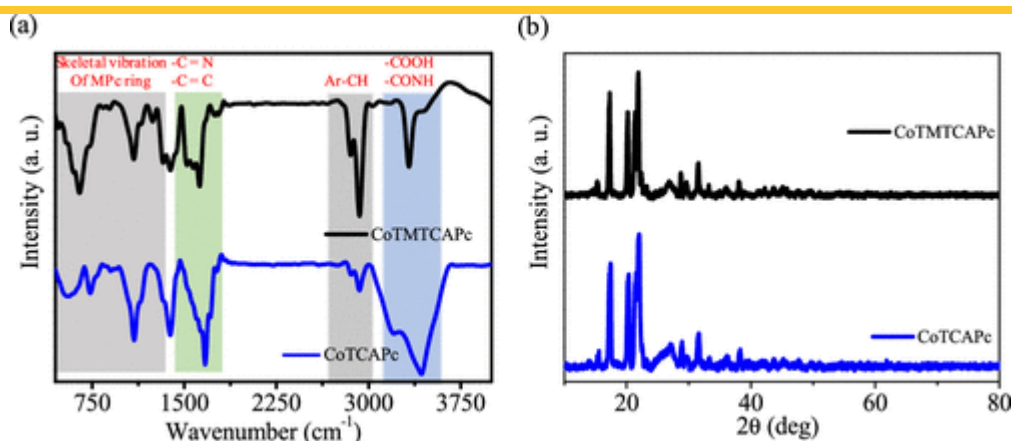
Publication Date (Web): March 5, 2026

[Abstract](#)

[Full text](#)

[PDF](#)

ABSTRACT



Correction to “Non-Precious Tetra-(4-methylthiazole)-carboxamide Cobalt(II) Phthalocyanine Supported on Functionalized Carbon Nanotubes as an Efficient Electrocatalyst for a Hydrogen Evolution Reaction”

Mounesh*, B. A. Thippeswamy, Pramod Shiralkar, R. Geetha Balakrishna, B. M. Nagaraja*, and K. Pramoda*

ACS Applied Energy Materials 2026, 9, 6, 3608-3609 (Addition/Correction)

Subscribed

Publication Date (Web): March 3, 2026

Full text

PDF

MASTHEADS

Issue Editorial Masthead

ACS Applied Energy Materials 2026, 9, 6, XXX-XXX (Article)

Subscribed

Publication Date (Web): March 23, 2026

PDF

Issue Publication Information

ACS Applied Energy Materials 2026, 9, 6, XXX-XXX (Article)

Subscribed

Publication Date (Web): March 23, 2026

PDF

READ

[Journals](#)

[Books & References](#)

[C&EN](#)

PUBLISH

[Submit a Manuscript](#)

[Author Resources](#)

[Peer Review](#)

[Purchase Author
Services](#)

[Explore Open Access](#)

Re

SUBSCRIBE

[Librarians & Account
Managers](#)

[Open Science for
Institutions](#)

[Inquire About Access](#)

HELP

[Support FAQ](#)

[Live Chat with Agent](#)

RESOURCES

[About ACS Publications](#)

[ChemRxiv](#)

[Blog](#)

[Events](#)

[Join ACS](#)

[For Advertisers](#)

1155 Sixteenth Street N.W.
Washington, DC 20036

[Copyright © 2026 American Chemical Society.](#)

[Terms of Use](#) [Privacy Policy](#) [Accessibility](#)

Advancing Interface Engineering for Non-Close-Packed Halide-Based All-Solid-State Lithium Batteries

Kai Zhang,[†] Songjia Kong,[†] Keqi Chen, Shumin Zhang,* Yanguang Li,* and Feipeng Zhao*



Cite This: *ACS Appl. Energy Mater.* 2026, 9, 2963–2974



Read Online

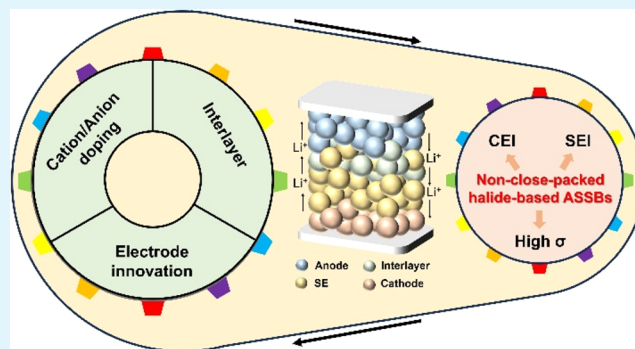
ACCESS |

Metrics & More

Article Recommendations

ABSTRACT: The growing demand for high-energy-density batteries has positioned all-solid-state lithium batteries (ASSBs) as a leading technology with the potential for significant impact. As a key material for ASSBs, halide solid electrolytes (SEs) have emerged as a current research hotspot, especially for non-close-packed halide SEs with ultrahigh ionic conductivity ($>10 \text{ mS cm}^{-1}$ at room temperature). However, they still suffer from insufficient compatibility with high-voltage cathode materials ($>4.3 \text{ V vs Li/Li}^+$) and poor reduction limit ($>0.9 \text{ V vs Li/Li}^+$). Based on the recent advancements, those challenges have been alleviated through cation/anion regulation engineering and the introduction of extra interlayers. This review distinguishes itself from previous works by systematically examining interfacial failure mechanisms and modification strategies for emerging non-close-packed halide SEs. Surpassing conventional halide SEs with close-packed structures, the non-close-packed ones enable broader cationic/anionic doping versatility, including multi-element co-doping and facilitate the improvement of interfacial engineering through more diverse interlayers. This focused review is expected to inspire more research on improving the interfacial stability between non-close-packed halide SEs and electrode materials, which would promote the development of high-performance ASSBs.

KEYWORDS: halide solid electrolytes, all-solid-state batteries, interfaces, element doping, non-close-packed structure



1. INTRODUCTION

To meet the growing energy demands of various electrical products, the development of secondary batteries with high energy density and long cycle life has become an urgent requirement. Currently, the energy density of lithium-ion batteries is gradually approaching a bottleneck (approximately 270 Wh kg^{-1}).¹ Meanwhile, their occasional safety incidents, such as thermal runaway and flammability, have hindered their large-scale practical applications.^{2,3} ASSBs have emerged as promising candidates to address these challenges, offering high energy density,^{4,5} long cycle life, and enhanced safety.^{6–8}

Based on differences in chemical composition, inorganic SEs can be categorized into three major types: oxides,⁹ sulfides,^{10,11} and halides.^{12,13} One of the key criteria for evaluating SEs is ionic conductivity. Sulfides have long been known for their high ionic conductivity; however, its electrochemical stability window (ESW) is relatively narrow. While traditional halide SEs were limited by their moderate ionic conductivity, non-close-packed halides exhibit ionic conductivities rivaling those of sulfides.^{8,14–16} Most non-close-packed halides show specific configurations where cations/anions are loosely arranged and leave significant voids. This feature is distinct from traditional close-packed halide SEs in which ions stack densely to form

crystals (Figure 1). The non-close-packed structure and weak van der Waals interactions between building blocks provide wide channels for ionic migration, while the “soft cradle effect” enables the spatiotemporal correlation between building anions (e.g., $[\text{TaO}_2\text{Cl}_4]^{3-}$) and lithium-ion hopping, reducing the migration energy barrier.¹⁷ Facilitated by these structural features, non-close-packed halide SEs achieve superior ionic conductivities, exemplified by LiNbOCl_4 for 10.4 mS cm^{-1} ,¹⁴ LiTaOCl_4 for 12.4 mS cm^{-1} ,¹⁴ and $\text{Li}_3\text{Ta}_3\text{O}_4\text{Cl}_{10}$ for 13.7 mS cm^{-1} .¹⁵

Beyond ionic conductivity, interfacial stability has emerged as a significant factor governing battery performance.^{18,19} In general, the oxidative stability of SEs follows the order of chlorides $>$ oxides $>$ sulfides, whereas the reductive stability decreases in the order of oxides $>$ sulfides $>$ chlorides.²⁰ Although many oxide SEs exhibit a favorable ESW,⁹ their

Received: December 22, 2025

Revised: February 24, 2026

Accepted: February 25, 2026

Published: March 3, 2026



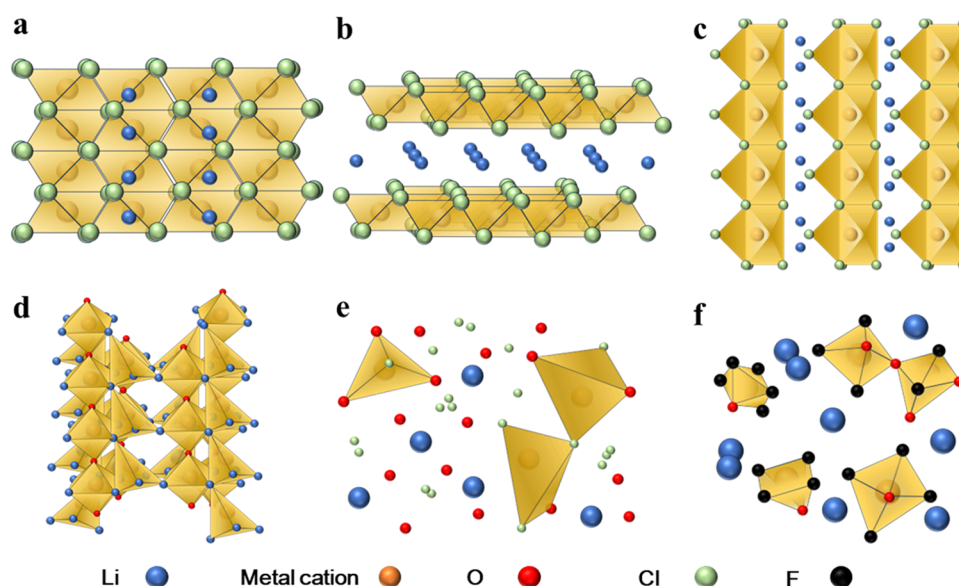


Figure 1. Schematic illustration of different halide structures. (a) Hexagonal close-packed type, (b) Cubic close-packed type, (c) UCl_3 type, (d) $\text{Cmc}2_1$ LiNbOCl_4 , (e) Amorphous LiAlOCl_2 , and (f) Amorphous LiTaOF_5 .

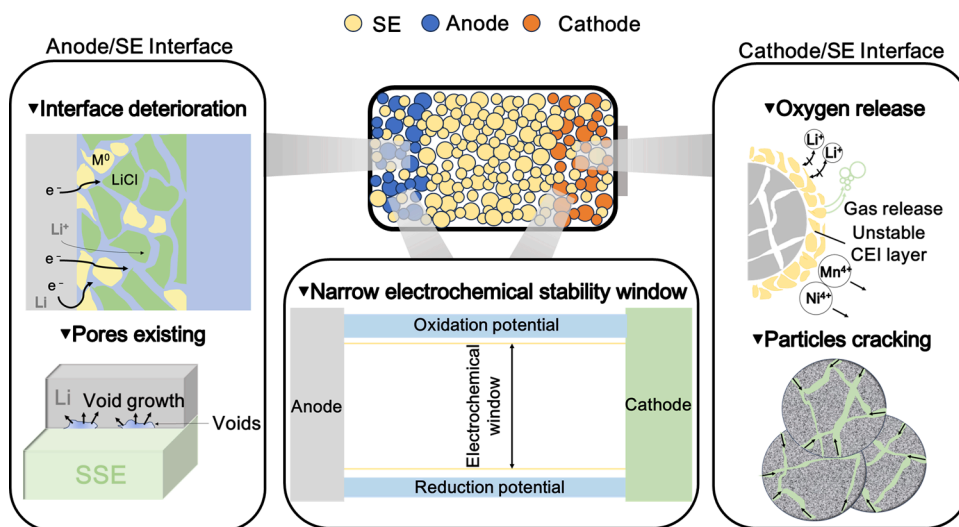


Figure 2. Schematic illustration of various interface issues in ASSBs.

practical application still faces challenges such as relatively low ionic conductivity and synthetic complexities.²¹ Sulfide-based SEs are constrained by a relatively low oxidation potential (approximately 2.5 V vs Li/Li^+) and poor chemical stability, being prone to decomposition reactions.²² This leads to severe interfacial side reactions when coupled with high-voltage cathode active materials (CAMs).^{23,24} By contrast, halide SEs, which demonstrate high oxidation potential (up to 6 V for fluorides), possess certain advantages in terms of oxidative stability.²⁵ Nevertheless, its performance in matching high-voltage cathodes and high-capacity anodes (e.g., Li, Si, P, etc.) still needs further improvement. Thermodynamically, high-valent metals in halide SEs tend to be reduced by lithium metal, forming high-impedance interfacial layers that impede ion transport. Furthermore, the cracking of SEs after prolonged cycles disrupts the intimate contact between SE and electrodes, leading to interfacial failure.

Previous studies have focused on summarizing the properties (e.g., ion transport, interfaces) of close-packed halides.^{26–29}

However, systematic reviews dedicated to non-close-packed halides remain scarce, despite their superior ionic conductivity and broad application prospects. In this review, we systematically elucidate the interfacial failure mechanisms of non-close-packed halide-based SEs and outline universal modification strategies. Through cation/anion regulation engineering, anode interlayer modification, and innovation of cathodes (particularly for halides), the interfacial side reactions have been effectively reduced for higher-performance requirements. Meanwhile, the strategies for interfacial modification can improve the cyclic lifespan of batteries while maintaining high ionic conductivity. This urgent summary not only provides valuable insights into the interfacial characteristics but also proposes some new strategies for the future optimization of halide-based SEs.

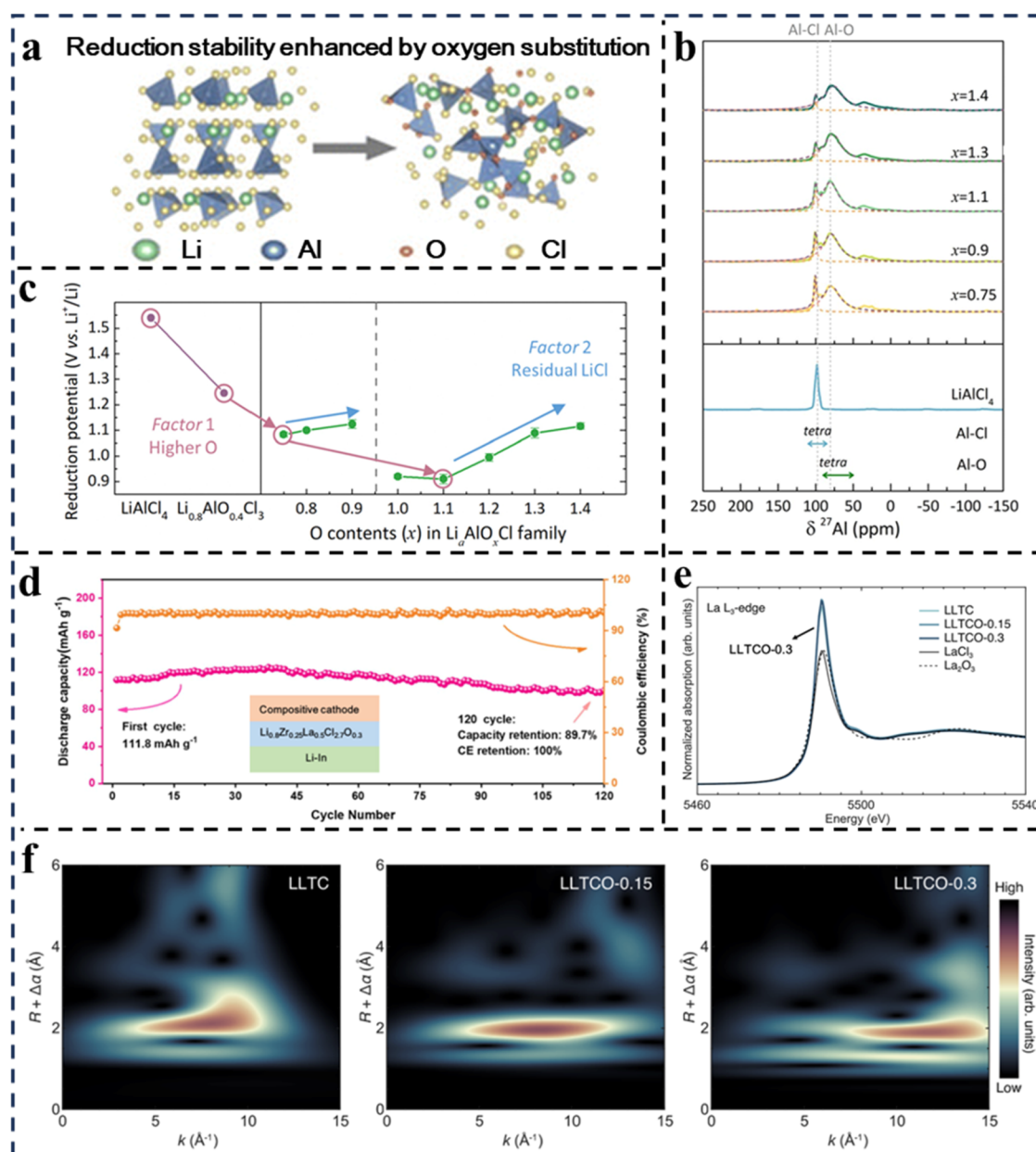


Figure 3. (a) Schematic illustration of reduction stability enhanced by oxygen substitution. Reproduced with permission from ref 20. Copyright 2025 Royal Society of Chemistry. (b) Deconvoluted ^{27}Al NMR spectra of Li–Al–O–Cl family with varying oxygen content. Dotted lines indicate the fitted peaks including peak indicating Al–Cl bond and Al–O bond. Reproduced with permission from ref 20. Copyright 2025 Royal Society of Chemistry. (c) The observed reduction onset potential of LiAlCl_4 , $\text{Li}_{0.8}\text{AlO}_{0.4}\text{Cl}_3$, and the Li–Al–O–Cl family depending on the O content (x). The two governing factors and error bars are indicated. Reproduced with permission from ref 20. Copyright 2025 Royal Society of Chemistry. (d) Corresponding long-term performance of discharge capacity and Coulombic efficiency of the ASSBs. Reproduced with permission from ref 51. Copyright 2024 Royal Society of Chemistry. (e) X-ray absorption near-edge structure for $\text{Li}_{0.388+x}\text{La}_{0.475}\text{Ta}_{0.238}\text{Cl}_{3-x}\text{O}_x$ ($x = 0, 0.15, 0.30$) SEs, as well as LaCl_3 and La_2O_3 at La L_3 -edge. Reproduced from ref 52. Copyright 2025 American Chemical Society. (f) Wavelet spectra of $\text{Li}_{0.388+x}\text{La}_{0.475}\text{Ta}_{0.238}\text{Cl}_{3-x}\text{O}_x$ ($x = 0, 0.15, 0.30$) SEs at Ta L_3 -edge with a k^3 weighting. Reproduced from ref 52. Copyright 2025 American Chemical Society.

2. MECHANISM OF INTERFACIAL FAILURES

2.1. Poor Reductive Stability

Lithium metal represents an ideal anode for high-energy-density energy storage due to its exceptionally low electrochemical potential (-3.045 V vs standard hydrogen electrode), low density (0.59 g cm^{-3}), and high theoretical specific capacity (3862 mAh g^{-1}).^{30,31} However, the relatively narrow ESW of halide SEs renders them vulnerable to interfacial degradation upon contact with electrode materials. Such interfacial

degradation deteriorates both battery performance and safety.^{32,33} In traditional halide SEs (e.g., Li_3YCl_6 , Li_3InCl_6), reductive decomposition at the lithium anode interface will generate electronic conductive phase (e.g., metal alloys), leading to continuous interfacial degradation.^{34–36} *In situ* XPS analysis revealed that In^{3+} in Li_3InCl_6 underwent reduction (to In metal), accompanied by LiCl formation, which generated a mixed ionic-electronic conductor interphase (MCI). Such MCI provides pathways for both Li^+ and electron transport, leading to continuous interfacial reactions and eventual failure. A similar

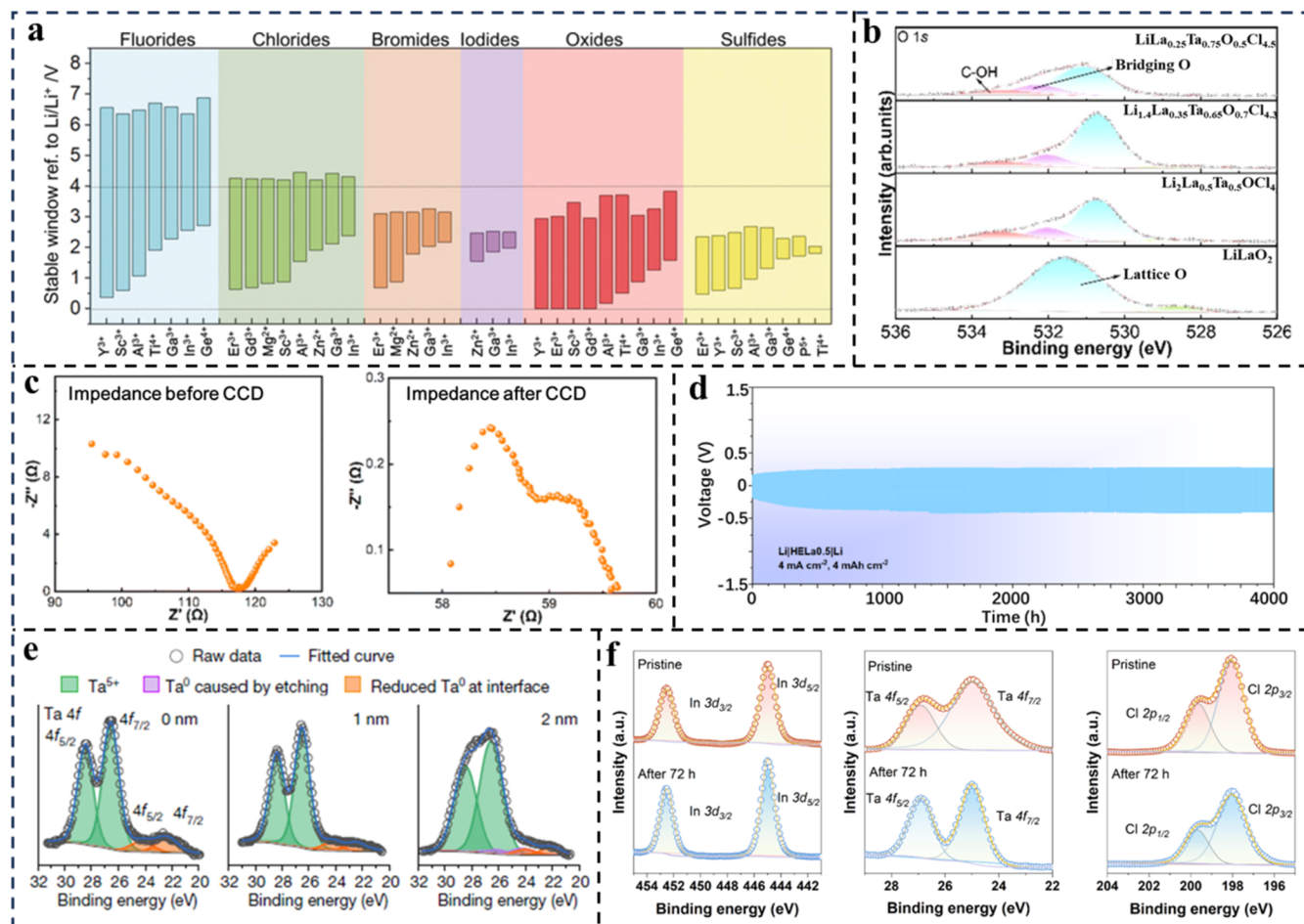


Figure 4. (a) Calculated thermodynamics intrinsic ESW of Li-M-X ternary fluorides, chlorides, bromides, iodides, oxides, and sulfides. M is a metal cation at its highest common valence state. Reproduced with permission from ref 53. Copyright 2019 Wiley-VCH. (b) O 1s XPS spectra of LiLaO_2 , $\text{LiLa}_{0.25}\text{Ta}_{0.75}\text{O}_{0.5}\text{Cl}_{4.5}$, $\text{Li}_{1.4}\text{La}_{0.35}\text{Ta}_{0.65}\text{O}_{0.7}\text{Cl}_{4.3}$, and $\text{Li}_2\text{La}_{0.5}\text{Ta}_{0.5}\text{OCl}_4$. Reproduced with permission from ref 54. Copyright 2025 Royal Society of Chemistry. (c) Nyquist profiles of the $\text{LiLi}_{1.4}\text{La}_{0.35}\text{Ta}_{0.65}\text{O}_{0.7}\text{Cl}_{4.3}$ symmetric battery before and after CCD. Reproduced with permission from ref 54. Copyright 2025 Royal Society of Chemistry. (d) Cycling performance of the $\text{Li/HELa}_{0.5}\text{Li}$ symmetric battery under a current density of 4 mA cm^{-2} and areal capacity of 4 mAh cm^{-2} . Reproduced with permission from ref 55. Copyright 2025 Elsevier. (e) Depth-dependent Ta 4f X-ray photoelectron spectroscopy (XPS) spectra of the interface of $\text{Li}_{0.388}\text{Ta}_{0.238}\text{La}_{0.475}\text{Cl}_3$ SE after 50 h of cycling. Note the inevitable partial reduction of Ta caused by etching that occurred during the depth analysis, along with the appearance of the new Ta 4f_{7/2} peak at 24.2 eV (purple). Reproduced with permission from ref 39. Copyright 2023 Springer Nature. (f) XPS spectra of the LiInTaCl solid electrolytes from the Stainless Steel/LPSCl/LiInTaCl/Stainless Steel cells after a static period of 72 h. Reproduced from ref 56. Copyright 2024 American Chemical Society.

issue occurs in Li_3YCl_6 (LYC), where an MCI (with Y nanoclusters and LiCl) aggravates failure.^{37,38} The chemical interaction between lithium metal and high-valence metals still dominates the interfacial degradation mechanism of non-close-packed halide SEs. The dominant decomposition product of some classic non-close-packed halides SE is LiCl, which serves as an electronic insulator and effectively blocks electron transfer, thereby precluding continuous interfacial reactions.³⁹ Additionally, lithium stripping during discharge creates interfacial voids that remain unfilled due to kinetic limitations. The resulting non-uniform current distribution promotes preferential lithium deposition around the void rather than void filling, which leads to further deteriorating the interfacial stability.^{18,40} However, in contrast to the conventional halide SEs, non-close-packed halide SEs exhibit improved anode compatibility through structural and compositional optimization. The enhanced stability of metal cations in the electrolyte lattice suppresses reductive decomposition and subsequent formation of conductive interphases. Nevertheless, long-term cycling stability remains inadequate, as side reactions related to metal reduction still occur during

prolonged charge-discharge cycles, limiting their practical application (Figure 2).⁸

2.2. High-Voltage Incompatibility

Halide SEs exhibit superior oxidation stability compared to sulfide and oxide counterparts, granting them inherent compatibility with cathode materials. However, interfacial challenges remain under high-voltage operation. Under high-voltage operation ($>4.3 \text{ V}$), halide SEs (except for fluorides) undergo oxidative decomposition, often initiating with the oxidation of halide anions (e.g., Cl^-) and the release of halogen gases. This process generates electrically insulating decomposition products, forming a resistive cathode-electrolyte interphase (CEI) that accelerates interfacial degradation.²⁶ For Ni-rich cathodes, high-voltage cycling ($>4.3 \text{ V}$) promotes the formation of residual lithium compounds and lattice oxygen release, which further destabilizes the interface. These reactions are exacerbated by the decomposition of the adjacent halide SEs, resulting in a cumulative degradation of the interfacial structure.^{41–43} Beyond electrochemical degradation, prolonged

cycling above 4.5 V induces cathode particle cracking via lattice strain accumulation,⁴⁴ ultimately causing mechanical separation (Figure 2).^{19,45–47} It is worth noting, however, that in non-close-packed halide frameworks, the stronger charge shielding effect provided by the structural configuration enhances the stability of anions against oxidation compared to conventional close-packed halide structures.⁴⁸ This effect partially mitigates the oxidative decomposition of the electrolyte at high voltages. Last but not least, conventional close-packed halide SEs typically display a high Young's modulus and increased rigidity.²⁴ When considering physical contact at the electrolyte-cathode interface, their performance is significantly inferior to that of softer, amorphous non-close-packed halide SEs.^{15,49,50} Thus, while halide SEs show promise for high-voltage applications, their interfacial stability remains a critical area for further improvement.

3. ENHANCEMENT OF INTERFACE STABILITY

3.1. Strategies toward Enhanced Interfacial Compatibility with Anodes

3.1.1. The Effect of Anion Engineering. Most halide SEs are engineered based on the general composition of Li-M-X, where M denotes one or more transition metals and X indicates halogen anions (F[−], Cl[−], Br[−], I[−]). Anion substitution, particularly with oxygen, serves as a primary strategy to modulate ESW and interfacial reactivity. For oxyhalides, Kim et al.²⁰ explored the cathodic stability of oxygen-incorporated Li–Al–Cl SEs. With increasing oxygen content, aluminum adopts more oxygen-rich coordination environments, leading to enhanced Al–O bonding at the expense of Al–Cl bonds (Figure 3a,b). This tendency to form chemical bonds with more electronegative elements results in the reductive onset potential changes from 1.54 V to 0.9 V. Specifically, for Li_xAlO_xCl₃ (1.0 ≤ *x* ≤ 1.6), the optimal ratio of *x* = 1.1 is crucial: at this juncture, the oxygen content sufficiently reduces the reductive onset potential to 0.9 V, while the LiCl content remains at a mere 18 wt % (Figure 3c). These resulting nanoscale LiCl particles (5–10 nm) are distributed embedded within amorphous matrix. Despite chemical inertness, these nanoparticles act as “nucleation centers” for reductive decomposition, which accelerates the reduction process of the surrounding matrix by lowering the nucleation barrier.

Building on this strategy, Cai et al.⁵¹ and Xu et al.⁵² improved the stability of the LaCl₃-based SEs in relation to the lithium-based anode through oxygen doping. When employing Li_{0.8}Zr_{0.25}La_{0.5}Cl_{2.7}O_{0.3} as the electrolyte and Li–In as the anode for ASSBs assembly, the cell can stably charge and discharge for over 120 cycles with a capacity retention of 89.7% (Figure 3d). More remarkably, Li_{0.538}La_{0.475}Ta_{0.238}Cl_{0.15}O_{0.15} electrolyte achieves ultralong cycling stability in the Li–Li symmetric cell (>4000 h at 10 mA cm^{−2} and 10 mAh cm^{−2}), with an overpotential below 1 V. These results collectively demonstrate that oxygen doping does not compromise the intrinsic functionality of the original cations (Figure 3e,f). It can also significantly enhance the lithium metal compatibility of SEs and effectively suppress the growth of lithium dendrites.

3.1.2. The Effect of Cation Engineering. In addition to the anion substitution, substituting the transition metal in Li-M-X is also a crucial approach to alleviate the anode interfacial issues of electrolytes. For halides, most of the metal cations will be reduced by the lithium anode (Figure 4a),⁵³ while the introduction of multiple cations is a viable method to mitigate

this issue. Similar to Li_{0.538}La_{0.475}Ta_{0.238}Cl_{0.15}O_{0.15}, Hu et al.⁵⁴ investigated the Li_{4x}La_xTa_{1−x}Cl_{5−2x}O_{2x} (*x* = 0.25, 0.35, and 0.5), enabling systematic tuning of five compositions, thereby overcoming the limitation of the study which only focused on a specific La/Ta ratio.⁵² For Li_{1.4}La_{0.35}Ta_{0.65}Cl_{4.3}O_{0.7}, an optimal cation doping ratio enables the maximization of the non-bridging oxygen/bridging oxygen ratio (Figure 4b). At an appropriate ratio, the material can achieve an exceptionally high critical current density (CCD). Under a current density of 40 mA cm^{−2}, the impedance at the electrolyte-anode interface exhibits a decreasing trend rather than short-circuiting (Figure 4c), demonstrating excellent compatibility between the electrolyte and the lithium metal anode. Meanwhile, the introduction of La³⁺ stabilizes the coordination environment of Ta⁵⁺ and inhibits its reduction to lower valence states (Ta³⁺). Structural characterization confirms homogeneous elemental distribution (La, Ta, O, Cl) without phase segregation, ensuring intimate interfacial contact that accommodates volume changes during cycling and prevents delamination.

Multi-cation doping strategies can be further extended to high-entropy electrolyte systems. Cai et al.⁵⁵ constructed the 0.5LiCl-*x*LaCl₃(TaCl₅·ZrCl₄·AlCl₃·CaCl₂)_{1/4(1−*x*)} (HEL*x*) (0.2 ≤ *x* ≤ 0.6) electrolyte. The amorphous phase introduced by multi-ion doping can optimize interfacial contact. In HELa0.5, the synergistic effect between the crystalline phase (providing 1D channels) and the amorphous phase (supplementing conduction paths) balances interfacial ion transport and structural stability. Consequently, the Li|HEL|Li symmetric cell achieves exceptional stability (>4000 h at 4 mA cm^{−2} and 4 mAh cm^{−2}), with an overpotential consistently below ±50 mV, which far surpasses that of traditional halide SEs (Figure 4d). In parallel, Yao et al.³⁹ have developed a universal LaCl₃-based SE, and conducted in-depth research on Li_{0.388}Ta_{0.238}La_{0.475}Cl₃. Compared with oxides that suffer from severe lithium dendrite issues, sulfides with poor areal capacity, and chlorides with inferior lithium compatibility, Li_{0.388}Ta_{0.238}La_{0.475}Cl₃ exhibits significantly advantageous high areal capacity and long cycle time. Benefiting from the structure of the framework LaCl₃, the symmetric battery can achieve stable cycling for over 5000 h under the conditions of 0.2 mA cm^{−2} and 1 mAh cm^{−2}. Unlike other SEs, it forms not only LiCl but also an interphase derived from metal gradient reduction at the interface (Figure 4e). Such an interphase is kinetically stable against lithium to a certain extent. Importantly, this framework is compatible with a variety of different cations, presenting broad application prospects, especially regarding Zr and Ca, due to their lower electronegativity compared with Ta. The cation-doped Li_{0.495}Zr_{0.259}Ca_{0.086}La_{0.432}Cl₃ exhibits enhanced oxidation resistance. Doping with more elements of low electronegativity is an effective approach to improving anode compatibility.

3.1.3. Interlayers. For most SEs, introducing an interlayer represents a viable strategy to improve interfacial compatibility between the SE and the anode.^{57,58} In conventional halide-based SEs, incorporating an Li₆PS₅Cl (LPSCI) interlayer has long been regarded as a classic approach to enhance anode compatibility; however, the inherent incompatibility between traditional halide SEs and LPSCI remains a significant limitation.^{59–61} In contrast, non-close-packed halide SEs exhibit markedly improved compatibility with LPSCI (Figure 4f), although their capacity for further optimization is constrained.⁶² For cation-doped non-close-packed halide SEs, the introduction of an LPSCI interlayer offers moderate isolation and protection, mitigating severe interfacial side reactions and thereby enhancing cycling

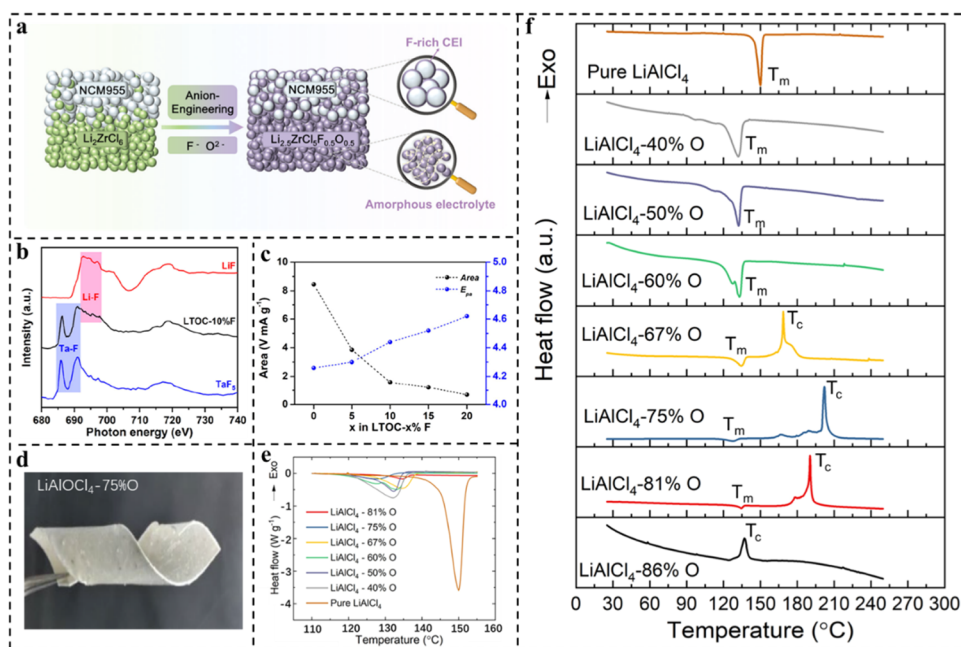


Figure 5. (a) Schematic representation of the role of LiF-rich CEI in enhancing the battery performance. Reproduced with permission from ref 34. Copyright 2024 Wiley-VCH GmbH. (b) F K-edge bulk XAS spectra of the LTOC-10%F SE, LiF, and TaF₅. Reproduced from ref 65. Copyright 2024 American Chemical Society. (c) The corresponding areas of the regions under the linear sweep voltammetry curves and the anodic peak potentials (E_{pa}); the dotted lines are guides for the eye. Reproduced from ref 65. Copyright 2024 American Chemical Society. (d) Winding membranes of LiAlCl₄-75%O (LiAlCl_{2.5}O_{0.75}, O/Al ratio of 75%, LACO) obtained by the rolling process. Reproduced with permission from ref 50. Copyright 2023 Springer Nature. (e) Enlarged endothermic peaks of LACO in the Differential Scanning Calorimetry (DSC) profiles for comparison. Reproduced with permission from ref 50. Copyright 2023 Springer Nature. (f) DSC heating profiles of LACO with different oxygen contents. Reproduced with permission from ref 50. Copyright 2023 Springer Nature.

stability.^{56,63} As mentioned previously, the electrolytes based on the LaCl₃ framework can form an interphase composed of LiCl and other reduced metal species, which can inhibit the continuous deterioration of the interface.³⁹ Nevertheless, this approach alone cannot fully resolve persistent anode interfacial challenges. Notably, in oxygen-doped non-close-packed SEs, oxygen species within the electrolyte can react with LPSCl to in situ form a Li₃PO₄ interphase layer situated between the LPSCl and the bulk electrolyte. This Li₃PO₄ layer exhibits high ionic conductivity, and its dense morphology effectively reduces charge transfer resistance while preventing the accumulation of insulating byproducts such as LiCl. Furthermore, the Li₃PO₄ interlayer acts as a chemical barrier that suppresses further reaction between the oxygen-containing halide and LPSCl, inhibits interfacial delamination, and preserves continuous ion transport pathways during prolonged cycling, thus significantly enhancing overall interfacial stability and compatibility.⁶²

3.2. Strategies toward Enhanced Cathode Compatibility of SEs

3.2.1. Anion Doping. While halide SEs exhibit relatively good cathode stability, their high-voltage stability requires further enhancement to meet performance demands. Unlike elemental doping strategies applied to the anode/SE interface, the doping effect not only determines the interfacial stability cathode/SE but also improves the intrinsic oxidation limit of the SEs. By co-doping with oxygen and fluorine, Zhang et al.³⁴ mitigated the cathode interfacial issues of LZC to some extent. The resulting Li_{2.5}ZrCl₃F_{0.5}O_{0.5} (LZCFO) forms a LiF-rich CEI, as illustrated in Figure 5a. TEM imaging reveals that the CEI formed between LZC and LiNi_{0.9}Co_{0.05}Mn_{0.05}O₂ (NCM955) is rough, non-uniform in thickness, and severely degraded. In

contrast, the LZCFO system produces a uniform, flat, and fluorine-rich CEI that completely coats the cathode particles. The fluorine-rich CEI considerably suppresses the oxidation of Cl⁻ when LZCFO is cycled at a high voltage of 4.35 V, enabling a capacity retention of 81.2% after 500 cycles. Moreover, a novel SE in the form of LiCl-4Li₂TiF₆ (LiCl-4LTF) is proposed by Jung et al.⁶⁴ This SE demonstrates exceptional oxidative stability up to 5.5 V (vs Li/Li⁺), although its ionic conductivity is relatively moderate (1.7×10^{-5} S cm⁻¹). When applied as a protective interlayer on CAMs, it suppresses side reactions and reduces interfacial resistance, thereby improving overall battery performance.

The lithium tantalum oxychlorides (LTOC) system also exhibits relatively favorable anodic stability after doping with more electronegative elements. Sun et al.⁶⁵ reported a series of amorphous LTOC-x%F ($x = 0, 5, 10, 15, 20$) SEs. Substitution of chloride ions by high-electronegative fluoride ions introduces Ta-F and Li-F bonds into the anionic framework (Figure 5b), significantly widening the ESW. As the fluorination degree increases, the high-voltage stability improves accordingly (Figure 5c). The optimized LTOC-10%F SE showed markedly enhanced high-voltage stability. During the first charge to 4.5 V, a LiF-rich CEI was in situ formed at the interface with LiCoO₂ (LCO), which isolated the LCO from the SE and prevented continuous interfacial reactions under high voltage, minimizing active material loss. The improved LTOC-10%F SE delivered a capacity retention of 81% after 300 cycles at 1.0 mA cm⁻² and 4.5 V, with an average Coulombic efficiency of 99.9%. For Ni-rich cathodes, LTOC can form a kinetically stable interface even without fluorine doping.⁶⁶ Notably, in LTOC-based ASSBs, lowering the operating temperature (e.g., -10 °C) significantly suppresses Co diffusion and interfacial reactions between high/

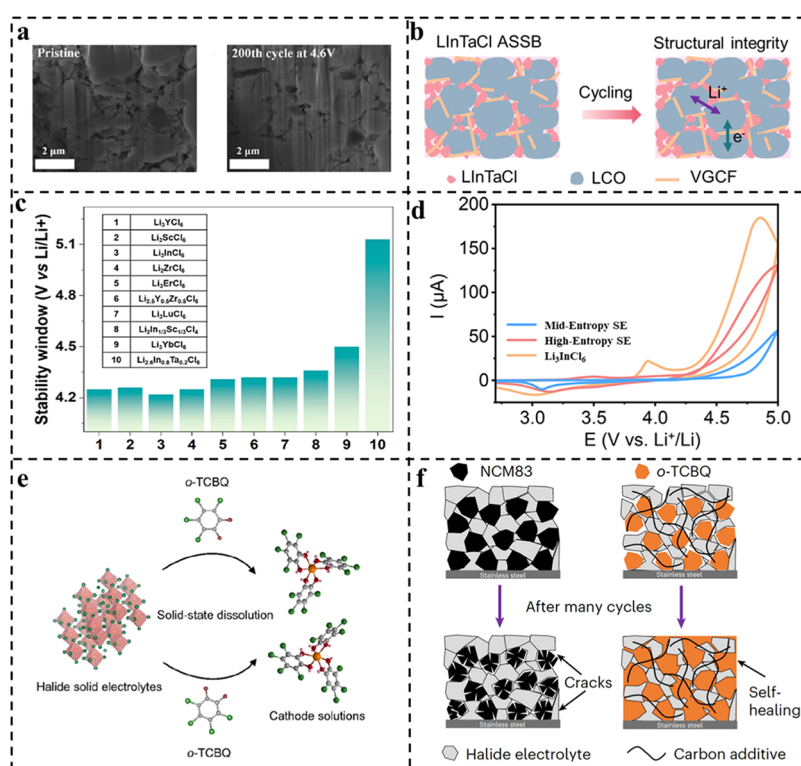


Figure 6. (a) Cross-sectional images of $\text{Li}_3\text{Nb}_{0.25}\text{Ta}_{0.75}\text{Cl}_5\text{OF}$ taken from focus-ion beam scanning electron microscopy for pristine at 1C between 3.0 V and 4.6 V and after 200th cycles at 1C between 3.0 V and 4.6 V. Reproduced with permission from ref 77. Copyright 2025 Elsevier. (b) Schematic illustrations of $\text{Li}_{2.6}\text{In}_{0.8}\text{Ta}_{0.2}\text{Cl}_6$ (LInTaCl) during cycling. Reproduced from ref 56. Copyright 2024 American Chemical Society. (c) Oxidation onset comparison with typical metal chloride SEs. Reproduced from ref 56. Copyright 2024 American Chemical Society. (d) CV curves of Mid-Entropy SE, compared with Li_3InCl_6 and High-Entropy SE. Reproduced with permission from ref 78. Copyright 2024 Springer Nature. (e) Solid dissolution feature of halide SEs in OEMs. Reproduced with permission from ref 80. Copyright 2025 Cell Press. (f) Schematic illustration of interfacial evolution in asymmetric $\text{Nb}^{5+}/\text{Al}^{3+}$ -based cathode solutions (right) and NCM83 (left) during cycling. Reproduced with permission from ref 81. Copyright 2025 Springer Nature.

medium-cobalt cathodes (LCO, NCM523) and LTOC, thereby greatly improving cycling stability. The recent low-temperature performance of $\text{Li}_3\text{Ta}_3\text{O}_4\text{Cl}_{10}$ shows an ionic conductivity of $5.68 \times 10^{-4} \text{ S cm}^{-1}$ even at -50°C . At 0.1C, it stably cycles for 2000 cycles, maintaining about 80 mAh g^{-1} with nearly 100% Coulombic efficiency, indicating strongly suppressed interfacial side reactions and far superior interfacial stability compared to liquid electrolytes.¹⁵

Similarly, in the oxygen-doping system, Al-based oxychlorides represent another promising class of cathode-compatible electrolytes. Li et al.⁶⁷ demonstrated that doping with oxygen anions induces the formation of “crystalline–amorphous composite structure.” The crystalline phases provide a highly conductive framework, while the amorphous phases adapt to electrode morphology via flexible polyanion structures, reducing interfacial gaps and contact resistance. Furthermore, Hu et al.⁵⁰ further observed that Al-based oxychloride SEs often exhibit polymer-like super plasticity, maintaining excellent interfacial contact (Figure 5d). DSC curves reveal that oxygen doping with varying oxygen contents significantly influences the physico-chemical properties (Figure 5e,f).

Consistent with the above, oxygen doping strategies have also achieved certain effects in improving the cathode compatibility of Zr-based halide SEs. Quasi-crystalline halide SEs (e.g., LZC) possess ordered crystalline structures but exhibit poor chemical compatibility with cathodes, leading to interfacial charge-transfer reactions. In contrast, amorphous oxyhalides such as $\text{Li}_3\text{ZrCl}_4\text{O}_{1.5}$ ⁴⁹ and other similar SEs^{68,69} with structural disorder

induced by oxygen incorporation show reduced chemical reactivity toward cathodes and enhanced performance. Li et al.⁷⁰ reported that modified $\text{Li}_{2.1}\text{Zr}_{0.95}\text{Cu}_{0.05}\text{Cl}_{4.4}\text{O}_{0.8}$ exhibits improved oxidation stability due to oxygen incorporation, with minimal Cl oxidation, thereby suppressing side reactions.

3.2.2. Cation Doping. Cation doping is widely used to modify halide SEs. Doping with Zr^{4+} , Ta^{5+} , and Al^{3+} can enhance ionic conductivity,^{71–73} given that aliovalent doping modulates lithium vacancy concentration, while isovalent doping optimizes unit cell volume.^{72,74} Additionally, Zr^{4+} and Y^{3+} doping enhances performance while also contributing to reduced production costs.⁷⁵ More importantly, cation doping has proven feasible in improving cathode compatibility. In the case of Al^{3+} doping, a lower Young’s modulus and increased amorphous degree result, leading to enhanced flexibility.⁷⁶ This greater flexibility allows for closer contact between the SE and the cathode, improving interfacial compatibility at the cathode-electrolyte interface. Cation doping with high-valent and highly electronegative metal cations has been demonstrated as an effective strategy to enhance cathodic oxidation stability. Huang et al.⁷⁷ reported a $\text{Li}_3\text{Nb}_x\text{Ta}_{1-x}\text{Cl}_5\text{OF}$ electrolyte in which Ta and Nb co-occupy lattice sites, leading to synergistic improvement in high-voltage stability. The optimized $\text{Li}_3\text{Nb}_{0.25}\text{Ta}_{0.75}\text{Cl}_5\text{OF}$ electrolyte elevates the oxidation potential from 4.08 V to 4.35 V. Structurally, this electrolyte comprises predominantly an amorphous $\text{Li}-\text{Ta}-\text{Nb}-\text{Cl}-\text{O}-\text{F}$ matrix with only trace amounts of secondary phases such as LiCl and LiF . This structural characteristic helps mitigate interfacial side reactions.

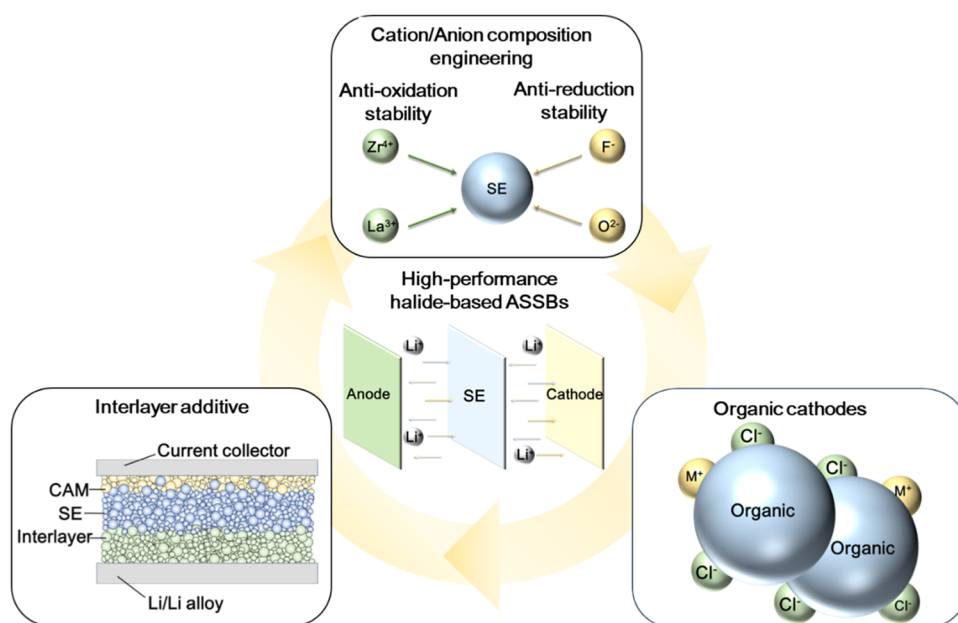


Figure 7. Schematic diagram of improvement schemes for non-close-packed halide SEs.

Notably, after cycling, interfacial voids are reduced, and more intimate contact is formed between the SE and the cathode, which contributes to improved battery performance (Figure 6a).

Wan et al.⁵⁶ achieved simultaneous enhancements by incorporating high-valent cations (Ta^{5+} , Nb^{5+}) into the Li_3InCl_6 lattice. Owing to the high electronegativity and strong bonding capability of Ta^{5+} , the oxidation onset voltage of $\text{Li}_{2.6}\text{In}_{0.8}\text{Ta}_{0.2}\text{Cl}_6$ is elevated to 5.13 V (vs Li^+/Li), significantly higher than the 4.22 V of the undoped material. Ta doping also leads to a significant suppression of interfacial decomposition after cycling (Figure 6b). When paired with an NCM811 cathode, the cell retains 70% capacity after 950 cycles at 4.4 V and 1C, markedly outperforming the undoped system, which suffers rapid capacity fade after 200 cycles and conventional liquid electrolytes that decompose under high voltage (Figure 6c). Additionally, the high-entropy strategy has been employed to enhance the high-voltage performance of SEs by incorporating five or more main-group metal elements. This approach leverages high configurational entropy to promote structural stability and modulate ion interactions. Likewise, Luo et al.⁷⁸ and Wagemaker et al.⁷⁹ demonstrated that high-entropy Li_3InCl_6 -based SEs exhibit significantly improved structural integrity and reduced interfacial side reactions with cathodes. ASSBs fabricated with these optimized electrolytes show substantially enhanced cycling stability under high-voltage conditions (Figure 6d).

3.2.3. Cathode Innovation. The innovative development of advanced halide SEs expedites the exploration of new cathode systems (e.g., organic cathodes) beyond conventional oxide-layer cathode materials.⁸² The use of organic cathodes enables enhanced cathode interfacial stability with advanced halide SEs, along with higher energy density and lower fabrication costs.^{81,83} In a recent work, Sun et al.⁸³ revealed a weak interaction between Zr-based SEs and phenanthrenequinone (PQ) organic cathode materials, specifically manifested by the formation of a weak Zr–O bond between the oxygen atoms in the C=O bonds of PQ and the Zr atoms in the SE. This weak interaction not only does not impair the lithium-ion transport capability of the electrolyte but also slightly increases the operating voltage of the

cathode. Meanwhile, it effectively suppresses the dissolution issue of the organic cathode.

Unfortunately, organic cathode materials also suffer from incompatibility with high operating voltages. To address this issue, the concept of using halide SEs as solid solutes and organic cathode materials as solid solvents has been proposed. Through rational design, the electrolyte and organic cathode form a homogeneous solid-state cathode solution, which is distinct from both traditional liquid-phase dissolution and the two-phase structure of composite electrolytes. The high-valent metal cations in the electrolyte, acting as Lewis acids, interact strongly with the carbonyl groups in the organic cathode (which function as Lewis bases), enabling stable dissolution (Figure 6e).^{80,81} Sun et al.⁸¹ designed a composite electrolyte with tetrachloro-o-benzoquinone (o-TCBQ) as the solid solvent and halides as the solutes. During the discharge process, o-TCBQ accepts electrons to form the electron-rich $[\text{C}_6\text{O}_2\text{Cl}_4]^{2-}$ moiety, which generates electrostatic interactions with metal cations (Nb^{5+} , Al^{3+}) in the halide SEs. These interactions drive the penetration of o-TCBQ molecules into the grain boundaries of the halide SEs, filling microcracks and thereby forming a solid solution. In the course of cycling, the interfacial impedance gradually decreases, indicating that the interfacial contact is continuously optimized with cycling (Figure 6f). Compared with traditional cathode materials, this composite electrolyte can operate stably under low stack pressure: it achieves 7570 cycles at a high rate of 5C with a capacity retention of 85%, and 6100 cycles at 10C with a capacity retention of 100%.

4. SUMMARY AND OUTLOOK

Our focused review examines interfacial challenges and corresponding solutions for non-close-packed halide SEs in ASSBs. Although halide SEs demonstrate superior oxidative stability compared to sulfide SEs and better processability than oxide SEs, their practical application is constrained by limited reduction stability and incompatibility with high-voltage cathodes.

To address interfacial issues at the anode and cathode, strategies including anion doping, cation regulation, and the

implementation of functional interlayers and innovative cathodes have been developed (Figure 7). These approaches effectively suppress the reductive activity of SEs, optimize lithium-ion transport pathways, and enhance interfacial stability while maintaining high ionic conductivity. Furthermore, they facilitate the formation of stable CEI layers, increase oxidation resistance, and mitigate parasitic side reactions, thereby enabling compatibility with high-voltage cathode materials. Beyond preserving ionic conductivity, these strategies significantly extend cycle life, providing critical pathways toward the practical implementation of halide SEs.

Future directions in this field are proposed as follow:

- (1) Stable operation with high-voltage cathodes represents the most critical challenge in advancing halide-based ASSBs. The design of halide-based cathodes that integrate redox activity, ionic conduction, and electronic transport within single-phase structures shows significant promise. These materials exhibit dynamic self-healing behavior through cation migration and mechanically adaptive phase transitions, effectively alleviating chemo-mechanical degradation.⁸⁴ Meanwhile, effective interfacial engineering strategies can mitigate side reactions and enable stable cycling with 4.5–5 V class cathode materials, addressing the compatibility challenges with high-voltage systems.⁸⁵
- (2) Expanding interfacial compatibility with high-capacity anode materials is equally essential for achieving superior energy density. The intrinsic flexibility of non-close-packed halide SEs could accommodate volume expansion in silicon and phosphorus anodes during cycling, thereby mitigating interfacial failure and capacity fading. Moreover, halide SEs demonstrate exceptional dynamic stability beyond their theoretical ESW, undergoing reversible lithiation/delithiation rather than irreversible decomposition. This mechanism improves interfacial ion transport with low-potential anodes while contributing additional capacity, laying a foundation for developing high-performance anode materials.⁸⁶
- (3) Supporting these interfacial engineering advances requires continued optimization of electrolyte material systems. Compositional tuning via fluorination represents a highly promising research direction as replacing Cl^- with F^- expands ESW to 0–6 V. This substitution forms metal cation-F/Li–F bonds that enhance compatibility with both high-voltage cathodes and lithium metal anodes while facilitating LiF-rich interfacial layer formation.^{65,85} Regulating the phase balance of amorphous–crystalline offers another critical direction, as phase composition significantly impacts ionic transport kinetics and interfacial stability. Current research indicates that most nonclose-packed halide SEs are predominantly amorphous, yet crystalline phases are inevitably incorporated as secondary constituents.^{8,13} Accordingly, elucidating the quantitative correlations between phase characteristics and interfacial stability remains a critical and worthy focus for advancing material design.
- (4) Translating these fundamental advances into commercial applications necessitates the development of scalable manufacturing processes for pouch cell fabrication. Wet film formation demands systematic investigation of doping strategies in solvent environments to ensure scalable wet-processing compatibility. Dry film formation requires achieving ultrathin films with robust mechanical performance through rational elemental doping, which is critical for high density and excellent flexibility. The superior doping flexibility of nonclose-packed halide SEs positions them favorably for large-scale commercialization of safe, cost-effective, and long-cycle-life pouch cells.^{87,88}

AUTHOR INFORMATION

Corresponding Authors

Shumin Zhang – Jiangsu Key Laboratory for Advanced Negative Carbon Technologies, Soochow University, Suzhou 215123, China; School of Physical Science and Technology, Jiangsu Key Laboratory of Frontier Material Physics and Devices, Suzhou Key Laboratory of Intelligent Photoelectric Perception, Center for Energy Conversion Materials & Physics (CECMP), Soochow University, Suzhou 215006, China; Email: szhang788@suda.edu.cn

Yanguang Li – Institute of Functional Nano & Soft Materials (FUNSOM), Soochow University, Suzhou 215123, China; Jiangsu Key Laboratory for Advanced Negative Carbon Technologies, Soochow University, Suzhou 215123, China; orcid.org/0000-0003-0506-0451; Email: yanguang@suda.edu.cn

Feipeng Zhao – Institute of Functional Nano & Soft Materials (FUNSOM), Soochow University, Suzhou 215123, China; Jiangsu Key Laboratory for Advanced Negative Carbon Technologies, Soochow University, Suzhou 215123, China; orcid.org/0000-0003-2686-6956; Email: feipeng@suda.edu.cn

Authors

Kai Zhang – Institute of Functional Nano & Soft Materials (FUNSOM), Soochow University, Suzhou 215123, China; Jiangsu Key Laboratory for Advanced Negative Carbon Technologies, Soochow University, Suzhou 215123, China

Songjia Kong – Department of Chemical Science and Engineering, School of Materials and Chemical Technology, Institute of Science Tokyo, Yokohama, Kanagawa 226-8502, Japan; orcid.org/0000-0002-3856-9388

Qeqi Chen – Institute of Functional Nano & Soft Materials (FUNSOM), Soochow University, Suzhou 215123, China; Jiangsu Key Laboratory for Advanced Negative Carbon Technologies, Soochow University, Suzhou 215123, China

Complete contact information is available at: <https://pubs.acs.org/10.1021/acsaem.5c04039>

Author Contributions

[†]K.Z. and S.K. contributed equally to this work.

Notes

The authors declare no competing financial interest.

ACKNOWLEDGMENTS

F.Z. acknowledged the research start-up funds from Soochow University and Jiangsu Specially-Appointed Professor Program. S.Z. acknowledged the support from the National Natural Science Foundation of China (52502293) and the Gusu Innovation and Entrepreneurship Leading Talent Program (ZXL2025331). The authors acknowledge the support from the Collaborative Innovation Center of Suzhou Nano Science and Technology.

REFERENCES

- (1) Frith, J. T.; Lacey, M. J.; Ulissi, U. A non-academic perspective on the future of lithium-based batteries. *Nat. Commun.* **2023**, *14*, No. 420.
- (2) Zhao, Q.; Stalin, S.; Zhao, C.-Z.; Archer, L. A. Designing solid-state electrolytes for safe, energy-dense batteries. *Nat. Rev. Mater.* **2020**, *5*, 229–252.
- (3) Janek, J.; Zeier, W. G. Challenges in speeding up solid-state battery development. *Nat. Energy* **2023**, *8*, 230–240.
- (4) Guo, J.-X.; Tang, W.-B.; Xiong, X.; Liu, H.; Wang, T.; Wu, Y.; Cheng, X.-B. Localized high-concentration electrolytes for lithium metal batteries: progress and prospect. *Front. Chem. Sci. Eng.* **2023**, *17*, 1354–1371.
- (5) Cui, G. Reasonable Design of High-Energy-Density Solid-State Lithium-Metal Batteries. *Matter* **2020**, *2*, 805–815.
- (6) Janek, J.; Zeier, W. G. A solid future for battery development. *Nat. Energy* **2016**, *1*, No. 16141.
- (7) Li, X.; Kim, J. T.; Luo, J.; Zhao, C.; Xu, Y.; Mei, T.; Li, R.; Liang, J.; Sun, X. Structural regulation of halide superionic conductors for all-solid-state lithium batteries. *Nat. Commun.* **2024**, *15*, No. 53.
- (8) Zhang, S.; Zhao, F.; Chen, J.; Fu, J.; Luo, J.; Alahakoon, S. H.; Chang, L.-Y.; Feng, R.; Shakouri, M.; Liang, J.; Zhao, Y.; Li, X.; He, L.; Huang, Y.; Sham, T.-K.; Sun, X. A family of oxychloride amorphous solid electrolytes for long-cycling all-solid-state lithium batteries. *Nat. Commun.* **2023**, *14*, No. 3780.
- (9) Murugan, R.; Thangadurai, V.; Weppner, W. Fast Lithium Ion Conduction in Garnet-Type $\text{Li}_7\text{La}_3\text{Zr}_2\text{O}_{12}$. *Angew. Chem., Int. Ed.* **2007**, *46*, 7778–7781.
- (10) Rayavarapu, P. R.; Sharma, N.; Peterson, V. K.; Adams, S. Variation in structure and Li⁺-ion migration in argyrodite-type $\text{Li}_6\text{PS}_3\text{X}$ (X = Cl, Br, I) solid electrolytes. *J. Solid State Electrochem.* **2012**, *16*, 1807–1813.
- (11) Kamaya, N.; Homma, K.; Yamakawa, Y.; Hirayama, M.; Kanno, R.; Yonemura, M.; Kamiyama, T.; Kato, Y.; Hama, S.; Kawamoto, K.; Mitsui, A. A lithium superionic conductor. *Nat. Mater.* **2011**, *10*, 682–686.
- (12) Li, X.; Liang, J.; Luo, J.; Banis, M. N.; Wang, C.; Li, W.; Deng, S.; Yu, C.; Zhao, F.; Hu, Y.; Sham, T.-K.; Zhang, L.; Zhao, S.; Huang, H.; Li, R.; Adair, K. R.; Sun, X. Air-stable Li_3InCl_6 electrolyte with high voltage compatibility for all-solid-state batteries. *Energy Environ. Sci.* **2019**, *12*, 2665–2671.
- (13) Singh, B.; Wang, Y.; Liu, J.; Bazak, J. D.; Shyamsunder, A.; Nazar, L. F. Critical Role of Framework Flexibility and Disorder in Driving High Ionic Conductivity in LiNbOCl_4 . *J. Am. Chem. Soc.* **2024**, *146*, 17158–17169.
- (14) Tanaka, Y.; Ueno, K.; Mizuno, K.; Takeuchi, K.; Asano, T.; Sakai, A. New Oxyhalide Solid Electrolytes with High Lithium Ionic Conductivity > 10 mS cm⁻¹ for All-Solid-State Batteries. *Angew. Chem., Int. Ed.* **2023**, *62*, No. e202217581.
- (15) Zhao, F.; Zhang, S.; Wang, S.; Reid, J.; Xia, W.; Liu, J.; King, G.; Kaduk, J.; Liang, J.; Luo, J.; Gao, Y.; Yang, F.; Zhao, Y.; Li, W.; Alahakoon, S.; Guo, J.; Huang, Y.; Sham, T.; Mo, Y.; Sun, X. Anion sublattice design enables superionic conductivity in crystalline oxyhalides. *Science* **2025**, *390*, 199–204.
- (16) Yue, J.; Zhang, S.; Wang, X.; Fu, J.; Xu, Y.; Weng, S.; Zhu, Y.; Zhao, C.; Zheng, M.; Wang, Y.; Zhu, X.; Wu, H.; Wang, G.; Xia, Y.; Cao, M.; Jing, Q.; Wang, X.; Xia, W.; Liang, J.; Sun, X.; Li, X. Universal superionic conduction via solid dissociation of salts in van der Waals materials. *Nat. Energy* **2025**, *10*, 1237–1250.
- (17) Jun, K.; Wei, G.; Yang, X.; Chen, Y.; Ceder, G. Exploring the soft cradle effect and ionic transport mechanisms in the LiMXCl_4 superionic conductor family. *Matter* **2025**, *8*, No. 102001.
- (18) Yoon, S. G.; Vishnugopi, B. S.; Nelson, D. L.; Yong, A. X. B.; Wang, Y.; Sandoval, S. E.; Thomas, T. A.; Cavallaro, K. A.; Shevchenko, P.; Alsag, E. P.; Wang, C.; Singla, A.; Greer, J. R.; Ertekin, E.; Mukherjee, P. P.; McDowell, M. Interface morphogenesis with a deformable secondary phase in solid-state lithium batteries. *Science* **2025**, *388*, 1062–1068.
- (19) Liu, H.; Wolfman, M.; Karki, K.; Yu, Y. S.; Stach, E. A.; Cabana, J.; Chapman, K. W.; Chupas, P. J. Intergranular Cracking as a Major Cause of Long-Term Capacity Fading of Layered Cathodes. *Nano Lett.* **2017**, *17*, 3452–3457.
- (20) Kim, W.; Han, S.; Lee, S.; Yoo, J.; Park, C.; Yu, S.; Won, D.; Lee, E.; Ko, K.-h.; Noh, J.; Choi, G.; Kim, M.; Kang, K. Oxygen-tuned aluminum-based halide solid electrolytes enabling low-voltage anode compatibility in all-solid-state batteries. *Energy Environ. Sci.* **2025**, *18*, 8039–8051.
- (21) Wang, Q.; Bai, N.; Wang, Y.; He, X.; Zhang, D.; Li, Z.; Sun, Q.; Sun, H.; Wang, B.; Wang, G.; Fan, L.-Z. Optimization and progress of interface construction of ceramic oxide solid-state electrolytes in Li-metal batteries. *Energy Storage Mater.* **2024**, *71*, No. 103589.
- (22) Ren, D.; Lu, L.; Hua, R.; Zhu, G.; Liu, X.; Mao, Y.; Rui, X.; Wang, S.; Zhao, B.; Cui, H.; Yang, M.; Shen, H.; Zhao, C.-Z.; Wang, L.; He, X.; Liu, S.; Hou, Y.; Tan, T.; Wang, P.; Nitta, Y.; Ouyang, M. Challenges and opportunities of practical sulfide-based all-solid-state batteries. *eTransportation* **2023**, *18*, No. 100272.
- (23) Ming, L.; Deng, M.; Li, S.; Jiang, Z.; Li, L.; Lu, Z.; Luo, Q.; Yang, J.; Cui, Z.; Yu, C. Reviving the ionic conductivity of air-unstable solid-state electrolytes via a facile heat treatment. *Chin. Chem. Lett.* **2025**, No. 111114.
- (24) Kim, K.; Park, D.; Jung, H.-G.; Chung, K. Y.; Shim, J. H.; Wood, B. C.; Yu, S. Material Design Strategy for Halide Solid Electrolytes Li_3MX_6 (X = Cl, Br, and I) for All-Solid-State High-Voltage Li-Ion Batteries. *Chem. Mater.* **2021**, *33*, 3669–3677.
- (25) Richards, W. D.; Miara, L. J.; Wang, Y.; Kim, J. C.; Ceder, G. Interface Stability in Solid-State Batteries. *Chem. Mater.* **2016**, *28*, 266–273.
- (26) Li, X.; Liang, J.; Yang, X.; Adair, K. R.; Wang, C.; Zhao, F.; Sun, X. Progress and perspectives on halide lithium conductors for all-solid-state lithium batteries. *Energy Environ. Sci.* **2020**, *13*, 1429–1461.
- (27) Kwak, H.; Wang, S.; Park, J.; Liu, Y.; Kim, K. T.; Choi, Y.; Mo, Y.; Jung, Y. S. Emerging Halide Superionic Conductors for All-Solid-State Batteries: Design, Synthesis, and Practical Applications. *ACS Energy Lett.* **2022**, *7*, 1776–1805, DOI: 10.1021/acsenergylett.2c00438.
- (28) Li, C.; Du, Y. Building a Better All-Solid-State Lithium-Ion Battery with Halide Solid-State Electrolyte. *ACS Nano* **2025**, *19*, 4121–4155.
- (29) Xu, R.; Wu, Y.; Dong, Z.; Zheng, R.; Song, Z.; Wang, Z.; Sun, H.; Liu, Y.; Zhang, L. Halide solid electrolytes in all-solid-state batteries: Ion transport kinetics, failure mechanisms and improvement strategies. *Nano Energy* **2024**, *132*, No. 110435.
- (30) Whittingham, M. S. History, Evolution, and Future Status of Energy Storage. *Proc. IEEE* **2012**, *100*, 1518–1534.
- (31) Aurbach, D.; Cohen, Y. The Application of Atomic Force Microscopy for the Study of Li Deposition Processes. *J. Electrochem. Soc.* **1996**, *143*, 3525–3532.
- (32) Umeshbabu, E.; Maddukuri, S.; Hu, Y.; Fichtner, M.; Munnangi, A. R. Influence of Chloride Ion Substitution on Lithium-Ion Conductivity and Electrochemical Stability in a Dual-Halogen Solid-State Electrolyte. *ACS Appl. Mater. Interfaces* **2022**, *14*, 25448–25456.
- (33) Fu, Y.; Ma, C. Interplay between Li_3YX_6 (X = Cl or Br) solid electrolytes and the Li metal anode. *Sci. China Mater.* **2021**, *64*, 1378–1385.
- (34) Shen, L.; Li, J. L.; Kong, W. J.; Bi, C. X.; Xu, P.; Huang, X. Y.; Huang, W. Z.; Fu, F.; Le, Y. C.; Zhao, C. Z.; Yuan, H.; Huang, J. Q.; Zhang, Q. Anion-Engineering Toward High-Voltage-Stable Halide Superionic Conductors for All-Solid-State Lithium Batteries. *Adv. Funct. Mater.* **2024**, *34*, No. 2408571.
- (35) Kwak, H.; Kim, J. S.; Han, D.; Kim, J. S.; Park, J.; Kwon, G.; Bak, S. M.; Heo, U.; Park, C.; Lee, H. W.; Nam, K. W.; Seo, D. H.; Jung, Y. S. Boosting the interfacial superionic conduction of halide solid electrolytes for all-solid-state batteries. *Nat. Commun.* **2023**, *14*, No. 2459.
- (36) Rosa, C.; Pesce, A.; Lannelongue, P.; Ravalli, M.; Lopez del Amo, J. M.; Lopez-Aranguren, P.; Quartarone, E.; Tealdi, C. Understanding interfacial stability and ionic transport in ethanol-synthesized Li_3InCl_6 solid electrolyte for all-solid-state batteries. *J. Phys. Chem. Solids* **2026**, *209*, No. 113327.

- (37) Riegger, L. M.; Schlem, R.; Sann, J.; Zeier, W. G.; Janek, J. Lithium-Metal Anode Instability of the Superionic Halide Solid Electrolytes and the Implications for Solid-State Batteries. *Angew. Chem., Int. Ed.* **2021**, *60*, 6718–6723.
- (38) Morino, Y.; Aoki, N.; Nakamoto, M. Revealing the Reductive Decomposition at the Interface of Li_3YCl_6 –Lithium Metal. *ACS Appl. Mater. Interfaces* **2025**, *17*, 45744–45751.
- (39) Yin, Y. C.; Yang, J. T.; Luo, J. D.; Lu, G. X.; Huang, Z.; Wang, J. P.; Li, P.; Li, F.; Wu, Y. C.; Tian, T.; Meng, Y. F.; Mo, H. S.; Song, Y. H.; Yang, J. N.; Feng, L. Z.; Ma, T.; Wen, W.; Gong, K.; Wang, L. J.; Ju, H. X.; Xiao, Y.; Li, Z.; Tao, X.; Yao, H. B. A LaCl_3 -based lithium superionic conductor compatible with lithium metal. *Nature* **2023**, *616*, 77–83.
- (40) Ning, Z.; Li, G.; Melvin, D. L. R.; Chen, Y.; Bu, J.; Spencer-Jolly, D.; Liu, J.; Hu, B.; Gao, X.; Perera, J.; Gong, C.; Pu, S. D.; Zhang, S.; Liu, B.; Hartley, G. O.; Bodey, A. J.; Todd, R. I.; Grant, P. S.; Armstrong, D. E.; Marrow, T. J.; Monroe, C. W.; Bruce, P. G. Dendrite initiation and propagation in lithium metal solid-state batteries. *Nature* **2023**, *618*, 287–293.
- (41) Dutta, J.; Ghosh, S.; Garlapati, K. K.; Martha, S. K. Chemical conversion of parasitic residual lithium compounds into beneficial artificial interface for cycle life improvement of $\text{LiNi}_{0.8}\text{Mn}_{0.1}\text{Co}_{0.1}\text{O}_2$ cathodes. *J. Power Sources* **2023**, *587*, No. 233717.
- (42) Wu, Z.; Zhang, C.; Yuan, F.; Lyu, M.; Yang, P.; Zhang, L.; Zhou, M.; Wang, L.; Zhang, S.; Wang, L. Ni-rich cathode materials for stable high-energy lithium-ion batteries. *Nano Energy* **2024**, *126*, No. 109620.
- (43) Zhang, X.; Wu, T.; Jian, J.; Lin, S.; Sun, D.; Fu, G.; Xu, Y.; Liu, Z.; Li, S.; Huo, H.; Ma, Y.; Yin, G.; Zuo, P.; Cheng, X.; Du, C. Dual Modification Strategy for Enhanced Cycling and Rate Performance of Ni-Rich Cathode Materials in Lithium-Ion Batteries. *Small* **2024**, *20*, No. 2404488.
- (44) Yan, P.; Zheng, J.; Gu, M.; Xiao, J.; Zhang, J.; Wang, C. Intragranular cracking as a critical barrier for high-voltage usage of layer-structured cathode for lithium-ion batteries. *Nat. Commun.* **2017**, *8*, No. 14101.
- (45) Li, J.; Zhou, Z.; Luo, Z.; He, Z.; Zheng, J.; Li, Y.; Mao, J.; Dai, K. Microcrack generation and modification of Ni-rich cathodes for Li-ion batteries: A review. *Sustainable Mater. Technol.* **2021**, *29*, No. e00305.
- (46) Lee, S.; Li, W.; Dolocan, A.; Celio, H.; Park, H.; Warner, J. H.; Manthiram, A. In-Depth Analysis of the Degradation Mechanisms of High-Nickel, Low/No-Cobalt Layered Oxide Cathodes for Lithium-Ion Batteries. *Adv. Energy Mater.* **2021**, *11*, No. 2100858.
- (47) Sun, H.-H.; Manthiram, A. Impact of Microcrack Generation and Surface Degradation on a Nickel-Rich Layered $\text{Li}[\text{Ni}_{0.9}\text{Co}_{0.05}\text{Mn}_{0.05}]\text{O}_2$ Cathode for Lithium-Ion Batteries. *Chem. Mater.* **2017**, *29*, 8486–8493.
- (48) Ai, F.; Lu, Y.-C. Coordination chemistry in advanced redox-active electrolyte designs. *Nat. Rev. Mater.* **2025**, *10*, 929–946.
- (49) Zhang, S.; Zhao, F.; Chang, L. Y.; Chuang, Y. C.; Zhang, Z.; Zhu, Y.; Hao, X.; Fu, J.; Chen, J.; Luo, J.; Li, M.; Gao, Y.; Huang, Y.; Sham, T.-K.; Gu, M. D.; Zhang, Y.; King, G.; Sun, X. Amorphous Oxyhalide Matters for Achieving Lithium Superionic Conduction. *J. Am. Chem. Soc.* **2024**, *146*, 2977–2985.
- (50) Dai, T.; Wu, S.; Lu, Y.; Yang, Y.; Liu, Y.; Chang, C.; Rong, X.; Xiao, R.; Zhao, J.; Liu, Y.; Wang, W.; Chen, L.; Hu, Y.-S. Inorganic glass electrolytes with polymer-like viscoelasticity. *Nat. Energy* **2023**, *8*, 1221–1228.
- (51) Hao, X.; Chen, K.; Jiang, M.; Tang, Y.; Liu, Y.; Cai, K. A novel LaCl_3 -based oxychloride solid-state electrolyte enables fast Li-ion transport and is compatible with lithium metal. *J. Mater. Chem. A* **2024**, *12*, 18459–18468.
- (52) Yang, J.; Chen, S.; Yuan, Q.; Tan, G.; Liu, Q.; Yang, S.; Deng, Y.; Zhao, Y.; Liu, W.; Yu, Y.; Cui, Y.; Wang, J.; Bo, S.-H.; Xu, C. UCl_3 -Type Crystalline Oxychloride Electrolytes for All-Solid-State Lithium-Ion Batteries. *J. Am. Chem. Soc.* **2025**, *147*, 36557–36569.
- (53) Wang, S.; Bai, Q.; Nolan, A. M.; Liu, Y.; Gong, S.; Sun, Q.; Mo, Y. Lithium Chlorides and Bromides as Promising Solid-State Chemistries for Fast Ion Conductors with Good Electrochemical Stability. *Angew. Chem., Int. Ed.* **2019**, *58*, 8039–8043.
- (54) Song, S.; Wei, F.; Xue, W.; Cui, Y.; Long, Z.; Shan, H.; Hu, N. Amorphous oxyhalide solid electrolytes with improved ionic conductivity and reductive stability for all-solid-state batteries. *J. Mater. Chem. A* **2025**, *13*, 26478–26486.
- (55) Hao, X.; Chen, K.; Jiang, M.; Tang, Y.; Liu, Y.; Cai, K. Multiplication doped LaCl_3 -based chloride solid-state electrolyte compatible with lithium metal. *Chem. Eng. J.* **2025**, *504*, No. 158963.
- (56) Ye, Y.; Geng, J.; Zuo, D.; Niu, K.; Chen, D.; Lin, J.; Chen, X.; Woo, H. J.; Zhu, Y.; Wan, J. High-Voltage Long-Cycling All-Solid-State Lithium Batteries with High-Valent-Element-Doped Halide Electrolytes. *ACS Nano* **2024**, *18*, 18368–18378.
- (57) Li, W.; Li, M.; Ren, H.; Kim, J. T.; Li, R.; Sham, T.-K.; Sun, X. Nitride solid-state electrolytes for all-solid-state lithium metal batteries. *Energy Environ. Sci.* **2025**, *18*, 4521–4554.
- (58) Di, L.; Huang, Z.; Gao, L.; Zuo, Y.; Zhu, J.; Sun, M.; Zhao, S.; Zheng, J.; Han, S.; Zou, R. Dynamic control of lithium dendrite growth with sequential guiding and limiting in all-solid-state batteries. *Sci. Adv.* **2025**, *11*, No. eadw9590.
- (59) Koç, T.; Hallot, M.; Quemain, E.; Hennequart, B.; Dugas, R.; Abakumov, A. M.; Lethien, C.; Tarascon, J.-M. Toward Optimization of the Chemical/Electrochemical Compatibility of Halide Solid Electrolytes in All-Solid-State Batteries. *ACS Energy Lett.* **2022**, *7*, 2979–2987.
- (60) Rosenbach, C.; Walther, F.; Ruhl, J.; Hartmann, M.; Hendriks, T. A.; Ohno, S.; Janek, J.; Zeier, W. G. Visualizing the Chemical Incompatibility of Halide and Sulfide-Based Electrolytes in Solid-State Batteries. *Adv. Energy Mater.* **2023**, *13*, No. 220367.
- (61) Samanta, S.; Bera, S.; Biswas, R. K.; Mondal, S.; Mandal, L.; Banerjee, A. Ionocovalency of the Central Metal Halide Bond-Dependent Chemical Compatibility of Halide Solid Electrolytes with $\text{Li}_6\text{PS}_5\text{Cl}$. *ACS Energy Lett.* **2024**, *9*, 3683–3693.
- (62) Zhang, H.; Yu, P.; Cui, Z.; Jin, H.; Tang, W.; Zhao, C.; Lei, J.; Liang, S.; Shi, Z.; Wang, J.; Li, Y.; Hussain, F.; Zhu, J.; Xia, W. Enhancing Compatibility of Halide with Sulfide-Electrolytes via High Oxygen Incorporation for Robust Solid-State Batteries. *Adv. Funct. Mater.* **2025**, *35*, No. e10497.
- (63) Li, R.; Lu, P.; Liang, X.; Liu, L.; Avdeev, M.; Deng, Z.; Li, S.; Xu, K.; Feng, J.; Si, R.; Wu, F.; Zhang, Z.; Hu, Y.-S. Superionic Conductivity Invoked by Enhanced Correlation Migration in Lithium Halides Solid Electrolytes. *ACS Energy Lett.* **2024**, *9*, 1043–1052.
- (64) Son, J. P.; Park, J.; Kim, H.-Y.; Kim, J.-S.; Song, Y. B.; Kim, C.; Kim, D.; Kim, J. S.; Lee, J.; Ko, S.; J. S.-J.; Choi, S.; Ahn, D.; Chae, K.; Kwon, G.; Wierzbicki, D.; Du, Y.; Lee, H.-W.; Seo, D.-H.; Nam, K.-W.; Jung, Y. Five-volt-class high-capacity all-solid-state lithium batteries. *Nat. Energy* **2025**, *10*, 1334–1346.
- (65) Gao, Y.; Zhang, S.; Zhao, F.; Wang, J.; Zhou, J.; Li, W.; Deng, S.; Fu, J.; Hao, X.; Li, R.; Sun, X. Fluorinated Superionic Oxychloride Solid Electrolytes for High-Voltage All-Solid-State Lithium Batteries. *ACS Energy Lett.* **2024**, *9*, 1735–1742.
- (66) Zhao, F.; Zhang, S.; Wang, S.; Andrei, C. M.; Yuan, H.; Zhou, J.; Wang, J.; Zhuo, Z.; Zhong, Y.; Su, H.; Kim, J. T.; Yu, R.; Gao, Y.; Guo, J.; Sham, T.-K.; Mo, Y.; Sun, X. Revealing unprecedented cathode interface behavior in all-solid-state batteries with oxychloride solid electrolytes. *Energy Environ. Sci.* **2024**, *17*, 4055–4063.
- (67) Wang, G.; Zhang, S.; Wu, H.; Zheng, M.; Zhao, C.; Liang, J.; Zhou, L.; Yue, J.; Zhu, X.; Xu, Y.; Zhang, N.; Pang, T.; Fu, J.; Li, W.; Xia, Y.; Yin, W.; Sun, X.; Li, X. Oxychloride Polyanion Clustered Solid-State Electrolytes via Hydrate-Assisted Synthesis for All-Solid-State Batteries. *Adv. Mater.* **2025**, *37*, No. e2410402.
- (68) Hu, L.; Wang, J.; Wang, K.; Gu, Z.; Xi, Z.; Li, H.; Chen, F.; Wang, Y.; Li, Z.; Ma, C. A cost-effective, ionically conductive and compressible oxychloride solid-state electrolyte for stable all-solid-state lithium-based batteries. *Nat. Commun.* **2023**, *14*, No. 3807.
- (69) Li, B.; Li, Y.; Zhang, H.-S.; Wu, T.-T.; Guo, S.; Cao, A.-M. Fast Li^+ -conducting Zr^{4+} -based oxychloride electrolyte with good thermal and solvent stability. *Sci. China Mater.* **2023**, *66*, 3123–3128.
- (70) Li, Z.; Mu, Y.; Lu, K.; Kang, G.; Yang, T.; Huang, S.; Wei, M.; Zeng, L.; Li, Y. Cation-Anion-Engineering Modified Oxychloride Zr-Based Lithium Superionic Conductors for All-Solid-State Lithium Batteries. *Angew. Chem., Int. Ed.* **2025**, *64*, No. e202501749.
- (71) Li, R.; Wen, S.; Xu, K.; Wang, C.; Lin, Z.; Tang, X.; Zhang, Z.; Hu, Y.-S. Ultrahigh Ionic Conductivity in Halide Electrolytes Enabled

by Anion Framework Flexibility Engineering. *J. Am. Chem. Soc.* **2026**, *148*, 3114–3127.

(72) Li, Y.-X.; Cui, L.-P.; Zhang, S.; Sun, P.-F.; Fang, C.-D.; Zhang, Y.-H.; Feng, L.-B.; Chen, J.-J. A high Al-doping ratio halide solid electrolyte with a 3D Li-ion transport framework. *EES Batteries* **2025**, *1*, 495–501.

(73) Huang, J.-Y.; Wen, Y.-C.; Lin, Y.-T.; Chu, P.-J.; Liu, Y.-S.; Wang, H.-Z.; Chang, Y.-P.; Hung, Y.-T.; Wei, D.-H.; Jin, B.-Y.; Liu, R.-S. Multifunctional Dual-Doping Strategy Improving Halide-Based Solid-State Electrolyte. *Adv. Energy Mater.* **2025**, *15*, No. e03135.

(74) Usami, T.; Tanibata, N.; Takeda, H.; Nakayama, M. Analysis of ion conduction behavior of Nb- and Zr-doped Li_3InCl_6 -based materials via material simulation. *APL Mater.* **2023**, *11*, No. 121107.

(75) Liu, S.; Zhou, L.; Neyts, K. From Promise to Production: Strategy for Halide-Based All-Solid-State Battery Pilot Lines. *Adv. Energy Mater.* **2025**, *16*, No. e05286.

(76) Zhang, S.; Xu, Y.; Wu, H.; Pang, T.; Zhang, N.; Zhao, C.; Yue, J.; Fu, J.; Xia, S.; Zhu, X.; Wang, G.; Duan, H.; Xiao, B.; Mei, T.; Liang, J.; Sun, X.; Li, X. A Universal Self-Propagating Synthesis of Aluminum-Based Oxyhalide Solid-State Electrolytes. *Angew. Chem.* **2024**, *63*, No. e202401373.

(77) Lin, Q.; Kang, X.; Li, L.; Yao, J.; Chen, Y.; Yan, X.; Yu, C.; Zhang, L.; Huang, Z. Enabling high-voltage stability and interface compatibility via Ta/Nb co-occupation in fluorinated Li-halide catholytes. *Energy Storage Mater.* **2025**, *75*, No. 104062.

(78) Song, Z.; Wang, T.; Yang, H.; Kan, W. H.; Chen, Y.; Yu, Q.; Wang, L.; Zhang, Y.; Dai, Y.; Chen, H.; Yin, W.; Honda, T.; Avdeev, M.; Xu, H.; Ma, J.; Huang, Y.; Luo, W. Promoting high-voltage stability through local lattice distortion of halide solid electrolytes. *Nat. Commun.* **2024**, *15*, No. 1481.

(79) Wang, Q.; Zhou, Y.; Wang, X.; Guo, H.; Gong, S.; Yao, Z.; Wu, F.; Wang, J.; Ganapathy, S.; Bai, X.; Li, B.; Zhao, C.; Janek, J.; Wagemaker, M. Designing lithium halide solid electrolytes. *Nat. Commun.* **2024**, *15*, No. 1050.

(80) Wang, Y.; Liang, J. Solid solvation structure design for advanced all-solid-state organic battery. *Matter* **2025**, *8*, No. 102458.

(81) Hu, Y.; Su, H.; Fu, J.; Luo, J.; Yu, Q.; Zhao, F.; Li, W.; Deng, S.; Liu, Y.; Yuan, Y.; Gan, Y.; Wang, Y.; Kim, J. T.; Chen, N.; Shakouri, M.; Hao, X.; Gao, Y.; Pang, T.; Zhang, N.; Jiang, M.; Li, X.; Zhao, Y.; Tu, J.; Wang, C.; Sun, X. Solid solvation structure design improves all-solid-state organic batteries. *Nat. Chem.* **2025**, *17*, 1313–1322.

(82) Zhang, S.; Zhao, F.; Li, L.; Sun, X. Solid-state electrolytes expediting interface-compatible dual-conductive cathodes for all-solid-state batteries. *Energy Environ. Sci.* **2025**, *18*, 6530–6539.

(83) Gao, Y.; Fu, J.; Hu, Y.; Zhao, F.; Li, W.; Deng, S.; Sun, Y.; Hao, X.; Ma, J.; Lin, X.; Wang, C.; Li, R.; Sun, X. Reviving Cost-Effective Organic Cathodes in Halide-Based All-Solid-State Lithium Batteries. *Angew. Chem., Int. Ed.* **2024**, *63*, No. e202403331.

(84) Fu, J.; Wang, C.; Wang, S.; Reid, J. W.; Liang, J.; Luo, J.; Kim, J. T.; Zhao, Y.; Yang, X.; Zhao, F.; Li, W.; Fu, B.; Lin, X.; Hu, Y.; Su, H.; Hao, X.; Gao, Y.; Zhang, S.; Wang, Z.; Liu, J.; Abdolvand, H.; Sham, T.-K.; Mo, Y.; Sun, X. A cost-effective all-in-one halide material for all-solid-state batteries. *Nature* **2025**, *643*, 111–118.

(85) Jin, H.; Wang, X.; Zhang, S.; Zhu, X.; Liu, C.; Yue, J.; Qu, J.; Wu, B.; Han, X.; Wang, Y.; Xu, Y.; Wu, H.; Zhou, L.; Zhang, M.; Lai, H.; Wang, S.; Liang, J.; Sun, X.; Li, X. Boosting ionic conductivity of fluoride electrolytes by polyanion coordination chemistry enabling 5 V-Class all-solid-state batteries. *Joule* **2026**, *10*, No. 102233.

(86) Cheng, Z.; Zhao, W.; Wang, Q.; Zhao, C.; Lavrinenko, A. K.; Vasileiadis, A.; Landgraf, V.; Bannenberg, L.; Li, Y.; Liang, J.; Liu, M.; Ganapathy, S.; Wagemaker, M. Beneficial redox activity of halide solid electrolytes empowering high-performance anodes in all-solid-state batteries. *Nat. Mater.* **2025**, *24*, 1763–1772.

(87) Forster, A. C.; Coskun, A. Challenges in Transitioning from Pellet to Practical Argyrodite-Based All-Solid-State Batteries. *ACS Energy Lett.* **2026**, *11*, 1100–1108.

(88) Ko, S.; Ue, M.; Yamada, A. A critical outlook for large-scale all-solid-state batteries. *Joule* **2026**, *10*, No. 102269.

学分认定推荐意见

纳米科学技术学院 24 级本科生张凯同学以共一第一身份在 *ACS Applied Energy Materials* 上发表题为 “*Advancing Interface Engineering for Non-Close-Packed Halide-Based All-Solid-State Lithium Batteries*” 的文章，本人知悉其论文创作全过程。该生负责了论文撰写的主要工作，成果真实有效，不存在挂名、代写等情况。在本次论文成果中，该生是论文的第一实际贡献人，充分体现出良好的本专业研究领域专业素养与科研能力。综上，该生成果合规有效，完全符合学分认定要求。本人特此推荐，同意张凯同学凭此推荐意见认定学分，恳请审核予以通过。

推荐老师：



2026 年 6 月 2 日

学分认定推荐意见

纳米科学技术学院 24 级本科生张凯同学以共一第一身份在 *ACS Applied Energy Materials* 上发表题为 “*Advancing Interface Engineering for Non-Close-Packed Halide-Based All-Solid-State Lithium Batteries*” 的文章，本人知悉其论文创作全过程。该生负责了论文撰写的主要工作，成果真实有效，不存在挂名、代写等情况。在本次论文成果中，该生是论文的第一实际贡献人，充分体现出良好的本专业研究领域专业素养与科研能力。综上，该生成果合规有效，完全符合学分认定要求。本人特此推荐，同意张凯同学凭此推荐意见认定学分，恳请审核予以通过。

推荐老师：



2026 年 6 月 2 日

创新创业学分认定诚信声明

本人郑重声明：所提交的用以申请创新创业学分认定的内容(包括但不限于学科竞赛获奖、学术论文、科研项目成果、专利创造成果、文学艺术类成果以及创业实践类成果等)均为本人在校期间原创取得，不存在任何侵权、造假等违规行为。

本人完全意识到本声明的法律后果由本人承担。本人所提交的内容如涉嫌违规违法，本人愿意承担相应后果。

申请人签名：张凯

指导（证明）老师签名：赵海鹏

2024年6月 3日

Record 1 of 1

Title: Advancing Interface Engineering for Non-Close-Packed Halide-Based All-Solid-State Lithium Batteries

Author(s): Zhang, K (Zhang, Kai); Kong, SJ (Kong, Songjia); Chen, KQ (Chen, Keqi); Zhang, SM (Zhang, Shumin); Li, YG (Li, Yanguang); Zhao, FP (Zhao, Feipeng)

Source: ACS APPLIED ENERGY MATERIALS **Volume:** 9 **Issue:** 6 **Pages:** 2963-2974 **DOI:** 10.1021/acsaem.5c04039 **Early Access Date:** MAR 2026 **Published Date:** 2026 MAR 23

Times Cited in Web of Science Core Collection: 0

Total Times Cited: 0

Usage Count (Last 180 days): 23

Usage Count (Since 2013): 23

Cited Reference Count: 88

Abstract: The growing demand for high-energy-density batteries has positioned all-solid-state lithium batteries (ASSBs) as a leading technology with the potential for significant impact. As a key material for ASSBs, halide solid electrolytes (SEs) have emerged as a current research hotspot, especially for non-close-packed halide SEs with ultrahigh ionic conductivity ($>10 \text{ mS cm}^{-1}$) at room temperature). However, they still suffer from insufficient compatibility with high-voltage cathode materials ($>4.3 \text{ V vs Li/Li}^+$) and poor reduction limit ($>0.9 \text{ V vs Li/Li}^+$). Based on the recent advancements, those challenges have been alleviated through cation/anion regulation engineering and the introduction of extra interlayers. This review distinguishes itself from previous works by systematically examining interfacial failure mechanisms and modification strategies for emerging non-close-packed halide SEs. Surpassing conventional halide SEs with close-packed structures, the non-close-packed ones enable broader cationic/anionic doping versatility, including multi-element co-doping and facilitate the improvement of interfacial engineering through more diverse interlayers. This focused review is expected to inspire more research on improving the interfacial stability between non-close-packed halide SEs and electrode materials, which would promote the development of high-performance ASSBs.

Accession Number: WOS:001706050600001

Language: English

Document Type: Review

Author Keywords: halide solid electrolytes; all-solid-state batteries; interfaces; element doping; non-close-packed structure

KeyWords Plus: DESIGN; BR; CL

Addresses: [Zhang, Kai; Chen, Keqi; Li, Yanguang; Zhao, Feipeng] Soochow Univ, Inst Funct Nano & Soft Mat FUNSOM, Suzhou 215123, Peoples R China.

[Zhang, Kai; Chen, Keqi; Zhang, Shumin; Li, Yanguang; Zhao, Feipeng] Soochow Univ, Jiangsu Key Lab Adv Negat Carbon Technol, Suzhou 215123, Peoples R China.

[Kong, Songjia] Inst Sci Tokyo, Sch Mat & Chem Technol, Dept Chem Sci & Engrn, Yokohama, Kanagawa 2268502, Japan.

[Zhang, Shumin] Soochow Univ, Ctr Energy Convers Mat & Phys CECMP, Jiangsu Key Lab Frontier Mat Phys & Devices, Sch Phys Sci & Technol, Suzhou Key Lab Intelligent, Suzhou 215006, Peoples R China.

Corresponding Address: Li, YG; Zhao, FP (corresponding author), Soochow Univ, Inst Funct Nano & Soft Mat FUNSOM, Suzhou 215123, Peoples R China.

Zhang, SM; Li, YG; Zhao, FP (corresponding author), Soochow Univ, Jiangsu Key Lab Adv Negat Carbon Technol, Suzhou 215123, Peoples R China.

Zhang, SM (corresponding author), Soochow Univ, Ctr Energy Convers Mat & Phys CECMP, Jiangsu Key Lab Frontier Mat Phys & Devices, Sch Phys Sci & Technol, Suzhou Key Lab Intelligent, Suzhou 215006, Peoples R China.

E-mail Addresses: szhang788@suda.edu.cn; yanguang@suda.edu.cn; feipeng@suda.edu.cn

Affiliations: Soochow University - China; Soochow University - China; Soochow University - China

Author Identifiers:

Author	Web of Science ResearcherID	ORCID Number
Zhao, Feipeng	AAR-7940-2020	
Li, Yanguang	A-2319-2014	0000-0003-0506-0451
Kong, Songjia	PUF-0989-2026	

Publisher: AMER CHEMICAL SOC

Publisher Address: 1155 16TH ST, NW, WASHINGTON, DC 20036 USA

Web of Science Index: Science Citation Index Expanded (SCI-EXPANDED)

Web of Science Categories: Chemistry, Physical; Energy & Fuels; Materials Science, Multidisciplinary

Research Areas: Chemistry; Energy & Fuels; Materials Science

IDS Number: FK8AD

ISSN: 2574-0962

29-char Source Abbrev.: ACS APPL ENERG MATER

ISO Source Abbrev.: ACS Appl. Energ. Mater.

Source Item Page Count: 12

Funding:

Funding Agency	Grant Number
Soochow University	NA
Collaborative Innovation Center of Suzhou Nano Science and Technology	NA

Gusu Innovation and Entrepreneurship Leading Talent Program	ZXL2025331
National Natural Science Foundation of China	52502293
Jiangsu Specially-Appointed Professor Program	NA

F.Z. acknowledged the research start-up funds from Soochow University and Jiangsu Specially-Appointed Professor Program. S.Z. acknowledged the support from the National Natural Science Foundation of China (52502293) and the Gusu Innovation and Entrepreneurship Leading Talent Program (ZXL2025331). The authors acknowledge the support from the Collaborative Innovation Center of Suzhou Nano Science and Technology.

Output Date: 2026-06-04

End of File